scientific reports

Check for updates

OPEN

Reference gene variability across age and sex in 5XFAD mice highlights normalization challenges in Alzheimer's models

Eleonora Daini, Kristy Antonioni, Monica Piemontese, Martina Bodria, Michele Zoli & Antonietta Vilella✉

Gene expression profiling in neurodegenerative diseases such as Alzheimer's Disease (AD) is frequently performed using real-time quantitative polymerase chain reaction (RT-qPCR). The accuracy of this technique relies heavily on selecting suitable reference genes (RGs) for normalization and internal control. Ideally, RGs should maintain consistent transcription levels, unaffected by cellular or pathological changes. However, identifying stable RGs is challenging, particularly in diseases like AD, where gene expression fluctuates across disease stages. This study aimed to determine the most stable RGs in two brain regions - cortex (CTX) and hippocampus (HIPP) - of male and female 5XFAD mice, a model of familial AD. The stability of five commonly used RGs namely Gapdh, Ppia, Rer1, Rpl27 and Rps29, was evaluated using GeNorm, NormFinder, BestKeeper, and EndoGene algorithms across three AD stages: prodromal (2 months of age, mo), early (4 mo), and late (7 and 10 mo). Results revealed region-, sex-, and time-dependent differences in RG expression stability, reflecting the distinct vulnerability of CTX and HIPP to Aβ pathology. Using the two most stable RGs for normalization improved precision, reducing variability and increasing the significance level in target gene expression analyses. These findings emphasize the necessity of validating RGs under specific experimental conditions to ensure reliable RT-qPCR quantification in AD research.

Keywords Reference genes, RT-qPCR, 5XFAD mice, Gene stability, Normalization, Alzheimer's disease

A variety of tools and techniques including metabolomic, proteomic, transcriptomic, and novel DNA sequencing strategies have been employed in studying disease-associated alterations and exploring intracellular pathways that could be affected by pathologies. To date, the most widely used method for the analysis of gene expression is represented by reverse transcription and real-time quantitative polymerase chain reaction (RT-qPCR). In fact, in neurodegenerative disorders such as Alzheimer's Disease (AD), RT-qPCR has served to identify gene expression changes related to the pathological status and/or disease-associated genes, being therefore key to uncover and understand the underlying mechanisms of this disease[1–4].

Unfortunately, AD-dependent changes in tissue composition, cell activity and fluctuation of mRNA synthesis make the identification of stable transcripts particularly difficult. So, ideally, at the experimental level an essential step is represented by the accurate identification of appropriate reference genes (RGs), whose expression must remain constitutively stable in all samples, in any experimental condition, regardless of the tissue type and possible disease state. However, it is clear that there is not a universal RG and careful evaluation and validation of several RGs is mandatory to identify reliable internal controls for data normalization.

Among transgenic AD models, the 5XFAD mouse is notable for its exceptionally rapid onset of amyloid pathology. By expressing five familial AD mutations, 5XFAD mice develop amyloid deposits as early as 2 months of age, with widespread plaque accumulation by 4–5 months[5]. This contrasts with other widely used models, such as 3XTg-AD, APP/PS1, and Tg2576, which exhibit slower pathology development, often not reaching significant amyloid deposition until 6–12 months of age. The accelerated progression in 5XFAD mice facilitates efficient study of early molecular changes, but also introduces pronounced alterations in cellular homeostasis, inflammation, and metabolism, which can affect the stability of commonly used RGs. Consequently, careful validation of RGs in this model is essential to ensure accurate normalization in gene expression studies.

Department of Biomedical, Metabolic and Neural Sciences, University of Modena and Reggio Emilia, Modena, Italy. ✉email: antonietta.vilella@unimore.it

In the literature of the past decades, in the vast majority of RT-qPCR experiments, constitutive genes referred to as "housekeeping genes" (HKGs), such as β-actin (Actb), glyceraldehyde-3-phosphate dehydrogenase (*Gapdh*), 18 S ribosomal RNA (*18 S*), ribosomal protein large P0 (*Rplp0*), have been used extensively as RGs in both physiological conditions and diseases like AD[6–10]. If on the one hand the use of HKGs is obvious given their basal cellular functions, on the other hand it has been demonstrated that their expression could be affected by disease-mediated changes in cell homeostasis and metabolism[11,12]. In this scenario, the use of HKGs to normalize target gene expression could lead to assessment errors, therefore overestimating, underestimating, or failing to recognize important biological effects. The need to assess the stability of these genes led to the development of advanced mathematical methods based on the analysis of multiple parameters. Among them, the most commonly used are delta cycle threshold (Ct) methods and the four algorithms GeNorm, NormFinder, BestKeeper and EndoGene Analyzer. The geometric mean of stability ranking, obtained with the different methods/algorithms, hereinafter referred to as consensus, can guide the identification of stable RGs.

In the 5XFAD mouse model of familiar AD, Gapdh[13] and Actb[14–16] genes have traditionally been used as reference for quantifying transcripts of interest, but the stability of these transcripts in this model has never been properly addressed. In addition, being AD a complex and progressive disease, sex and age could also affect stability but this aspect has also never been thoroughly investigated in this pathological model.

In this study, we report the comparative analysis of 5 commonly used RGs involved in different biological functions, namely Gapdh, Peptidylprolyl isomerase A (Ppia), Retention In Endoplasmic Reticulum Sorting Receptor 1 (Rer1) and ribosomal protein coding genes Rpl27 and Rps29, as putative RGs for RT-qPCR analysis in brain samples of 5XFAD mice compared to B6SJL control mice. The identification of the most stable genes was conducted in two brain areas - cortex (CTX) and hippocampus (HIPP) - differently affected by AD pathology, considering sex differences and phases of plaque maturation, i.s. prodromal (2 month-old (mo), early (4 mo), and advanced (7 and 10 mo)[17]. The two RGs identified as most stable for each condition were then used as normalizers to evaluate the expression of different targets - namely C-X3-C motif chemokine receptor 1, (*Cx3cr1*), C-X3-C motif chemokine ligand 1 (*Cx3cl1*), hexosaminidase B (H*exb*) and lipoprotein lipase 4 (*Lpl4*) - with normalization over the least stable gene and all the tested RGs as comparators.

Materials and methods

Experimental mouse model

The 5XFAD transgenic mouse model of AD co-overexpresses a triple-mutant human amyloid precursor protein (APP) (Swedish mutation: K670N, M671L; Florida mutation: I716V; London mutation: V717I) and a double-mutant human presenilin 1 (PS1) (M146L and L286V mutations) transcriptionally regulated by the neuron-specific Thy-1 promoter. Progenitors with no retinal degeneration allele Pde6brd1 were purchased from Jackson Laboratories (Bar Harbor, ME, USA) and progeny was obtained by crossing 5XFAD^{Het} mice with B6SJL breeders. Mice were kept in conditioned rooms with stable temperature (21 °C) and humidity (60%), on a light/dark cycle of 12 h with *ad libitum* food and water. 2, 4, 7 and 10 mo male and female 5XFAD^{Het} (hereinafter called only 5XFAD) and relative controls (B6SJL) were used. All animal procedures were approved by the Committee on Animal Health and Care of the University of Modena and Reggio Emilia (protocol number: n° 465/2025-PR and 445/2025-PR) and conducted in accordance with National Institutes of Health (NIH) guidelines.

Age selection rationale

We selected the ages of 2, 4, and 7–10 months because they represent distinct and well-characterized stages of pathology progression in the 5XFAD model. Early amyloid deposition and initial glial activation occur by 2 months, marking the onset of detectable pathology hallmarks. By 4 months, 5XFAD mice show robust accumulation of Aβ and pronounced neuroinflammatory activation, corresponding to the transition from early to established pathology. Finally, 7–10 months represent a stage of advanced amyloid burden and sustained transcriptional and cellular alterations. These stages are supported both by our group's phenotype characterization[17] and by independent behavioural[18], transcriptomic and histopathological studies that demonstrate major shifts in inflammatory, synaptic, and metabolic pathways between 1 and 4 months, with continued progression through 9–10 months[19].

RNA isolation and cDNA synthesis

At each experimental age, mice were deeply anesthetized with isoflurane and sacrificed through intracardiac injection of cold PBS, the brain was dissected and CTX and HIPP were homogenized by mechanical disruption in QIAzol reagent (Qiagen, #79306), RNA was isolated following the procedure provided by the manufacturer (RNeasy Plus Mini Kit, Qiagen, #74136) and processed for RT-qPCR as described below[20,21]. After isolation, the RNA amount and quality were assessed to ensure an accurate estimation of gene expression; specifically, 260/230 and 260/280 absorbance ratios of RNA samples were measured, and those with values ranging from 1.9 to 2.1 were used for the analysis (data not shown). In addition, the integrity of RNA was evaluated through denaturing gel electrophoresis as indicated in the MIQE guidelines[22]. The bands corresponding to 18 S rRNA and 28 S rRNA were observed (data not shown).

Isolated mRNA was reverse transcribed into 30 ng/µl cDNA using random hexamers and M – MLV Reverse Transcriptase (Promega Corporation) following the instructions provided by the manufacturer. Samples were heated at 70 °C for 5 min to eliminate any secondary structures, then incubated 10 min at 23 °C, 1 h at 37 °C, and 5 min at 95 °C before being chilled at 4 °C, using a thermocycler (SimpliAmp, Applied Biosystem).

Real time PCR analysis

RT-qPCR was conducted using CFX connect Bio-Rad RT-qPCR detection system. Each reaction consisted of 20 µl, with 10 µl of iTaq Universal SYBR Green Supermix (Bio-Rad, #1725124), 0.6 µl of each primer (300 nM final concentration) (Table 1), 1 µl of cDNA (30 ng) and 7.8 µl RNase free water. The PCR protocol consisted in the following cycling parameters: 2 min at 95 °C (incubation) and 40 cycles of 5 min at 95 °C (denaturation) and 30 s at 60 °C (annealing/extension) followed by 5 s at 95 °C and 65 to 95 °C (melting curve analysis). Reaction was carried out in a 96-well plate of white color allowing enhanced fluorescence signal detection and improved sensitivity.

Standard curves were automatically generated by Bio-Rad CFX Maestro software by plotting Ct value and Log of serial dilution of cDNA (7.5, 15, 30, 60 ng). Each reaction was performed in triplicate as described above. Table 1 provides a summary of gene symbol, name and function and primer sequences, melting temperature (Tm), efficiency and amplicon size.

In order to evaluate the variability of each candidate RG, Ct values were subtracted from the Ct of the least expressed sample (highest Ct) and the resulting exponential value was used to calculate the mean and standard deviation (SD). A coefficient of variation (CV) was obtained as a percentage value of the SD divided by the mean.

Evaluation of expression stability of candidate reference genes

All analyses were performed both keeping the sexes separated (male, female) and combining males and females. For each method used (described below), samples were analyzed (i) irrespective of genotype/age (all), (ii) grouped by genotype (B6SJL and 5XFAD) or, (iii) by age (2 mo, 4 mo, 7 mo, 10 mo).

For each gene/brain area, Ct values were obtained by applying a manual Threshold (Thr) corresponding to the mean of automatic baseline thresholds from different plates, as indicated in **Suppl.**Table 1.

Normfinder

Normfinder algorithm allows the identification of stable genes among a set of candidates, evaluating their variation between (intergroup) and within (intragroup) sample groups. Normfinder outputs a stability value for each candidate gene, which is lower the greater the expression stability is within the same group and among different groups. For each candidate RGs, Ct value duplicates were averaged and 2^{-DCt} was calculated, normalizing the mean Ct of each sample over the most expressed one (sample with lowest mean Ct)[23].

GeNorm

GeNorm tool calculates the average pairwise variation of a gene compared to all other candidates, by measuring SD of log-transformed expression ratios. Obtained M value is an index of stability, with genes with low M being more stable[24]. GeNorm analysis was performed on qBase+ software using qPCR Ct data files.

Gene symbol	Gene name	Gene function	Primer sequence (5'–3')	T_m	Amplicon length (bp)	E (%)	R^2
Gapdh	glyceraldehyde-3-phosphate dehydrogenase	energy metabolism	CAAGGTCATCCATGACAACTTTG	58.2	90	98.3	0.997
			GGGCCATCCACAGTCTTCTG	60.39			
Ppia	peptidylprolyl isomerase A	isomerization of prolyl residues in peptides	AGCATACAGGTCCTGGCATC	59.53	127	85	0.999
			TTCACCTTCCCAAAGACCAC	57.64			
Rer1	retention in endoplasmic reticulum sorting receptor 1	endoplasmic reticulum receptor	CCACCTAAACCTTTTCATTGCG	58.43	159	91.4	0.993
			TTTGTAGCTGCGTGCCAAAAT	63.63			
Rpl27	ribosomal protein L27	ribosome component	ACATTGACGATGGCACCTC	57.84	111	97	0.998
			GCTTGGCGATCTTCTTCTTG	57.18			
Rps29	ribosomal protein S29	ribosome component	TGAAGGCAAGATGGGTCAC	57.35	127	95.9	0.997
			GCACATGTTCAGCCCGTATT	58.91			
Cx3cl1	chemokine (C-X3-C motif) ligand 1	regulation of microglia	CATCCGCTATCAGCTAAACCAG	58.94	66	102.6	0.995
			TGCTGTGTCGTCTCCAGGAC	61.81			
Cx3cr1	chemokine (C-X3-C motif) receptor 1	regulation of microglia	ACGGAGACAGTGGCGTTCAG	62.42	109	62	0.999
			CGGCCAGGCACTTCCTATAC	60.25			
Hexb	hexosaminidase B	energy metabolism	CTCGAGTCAGAGTGCGAGTC	59.9	120	101.1	0.997
			TAAACCTCGTAACGCTCCCC	59.47			
Lpl4	lipoprotein lipase	lipid metabolism	GGATGGACGGTAACGGGAAT	59.53	168	98	0.995
			GGCCACATCATTTCCCACCA	60.61			

Table 1. Overview of candidate RGs and targets and corresponding primer pairs for RT-qPCR. Amplicon length and Tm were assessed using NIH primer blast while primer efficiency and R^2 were calculated using at least four points on the standard curve. **Abbreviations**: E: efficiency; bp: base pair, length of the amplicon; T_m: melting temperature [°C].

BestKeeper
The Excel-based tool BestKeeper allows the determination of the most stable gene among a set of candidates by using repeated pair-wise correlation analysis and calculating the SD and the coefficient of variance[25]. Ct mean values for each sample/gene were analyzed using this tool irrespective of group separation.

EndoGene analyzer
EndoGene Analyzer is an online utility that can be accessed through NPO website[26] (https://npobioinfo.shinyapps.io/endogeneanalyzer/). This analysis was performed on mean Ct value for each sample/gene and SD of each candidate gene was recorded as a parameter of stability. Candidates with lower SD were considered more stable.

Consensus
Following each analysis, a ranking was assigned to each candidate gene based on its stability compared to the other genes, from 1 being the most stable to 5 the least stable. To detect the most stable couple of genes considering all different methods, a consensus value was calculated for each candidate gene as the geometric mean of the ranking score obtained in the 4 different analyses.

Comparative analyses
A comparative analysis was performed to assess the variability of candidate reference genes dependent on AD progression. To this purpose, for each candidate RG 2^{-DCt} was calculated normalizing Ct of 5XFAD samples to the mean Ct of the age-matched B6SJL mice. Additionally, mice of different experimental ages were analyzed normalizing each genotype over 2 mo B6SJL (for 4, 7 and 10 mo B6SJL) or 2 mo 5XFAD (for 4, 7 and 10 mo 5XFAD) mice.

Finally, RG variation was evaluated for each experimental age, by normalizing the Ct of each sample to the mean Ct of the 2 most stable (2MS) genes (DCt), identified in consensus analysis, and calibrating this value to the mean DCt of B6SJL group (DDCt).

Reference gene validation
To validate the impact of RG choice in RT-qPCR normalization, the expression of four target genes was analyzed in both CTX and HIPP between age-matched B6SJL and 5XFAD male and female mice. Data were normalized to distinct sets of RGs: (i) the two candidate RGs that in our analysis displayed the highest stability (2MS) and (ii) the lowest stability (least stable RG, LS) and (iii) all analyzed RGs (A). Gene expression changes were analyzed by means of 2^{-DDCt} method[27].

Data analysis and statistics
Data are presented as mean ± SD. For statistics, data were analyzed with univariate ANOVA or repeated measure ANOVA using SPSS (version 20), considering p value (p) ≤ 0.05 as threshold for significance. Graphs were plotted using Graph-Pad Prism (v10).

Results
Assessment of amplification efficiency and primer specificity
For each candidate RG, the efficiency of primers was calculated and ranged between 85.0% (*Ppia*) and 98.3% (*Gapdh*) using four points on the standard curve with R^2 -values ranking from 0.993 (Rer1) to 0.999 (Ppia) (Table 1). Melting curve analysis was performed between 65 °C and 95 °C resulting in a single peak suggesting the amplification of a single product and the absence of primer dimer formation (**Suppl. Figure 1**); in addition, PCR product electrophoresis showed a single band with the expected amplicon length (**Suppl. Figure 2**) with the blank control displaying no detectable signal (not shown).

Effect of AD progression on reference gene expression in both male and female mice
To evaluate the stability of candidate RGs across the different experimental conditions, an equal amount of cDNA (30 ng) was used as template for qPCR analysis. For each sample, the Ct values of *Gapdh*, *Ppia*, *Rer1*, *Rpl27* and *Rps29* in CTX and HIPP of B6SJL and 5XFAD mice at the 4 ages studied were analyzed considering male and female mice separated as well as together. As shown in Fig. 1, the expression level of the five candidate RGs demonstrated a wide range of variability; in both analyzed areas, *Rpl27* showed the lowest expression level ($Ct_{mean\ CTX}$ = 22.198; $Ct_{mean\ HIPP}$ = 22.614) followed by *Rer1* ($Ct_{mean\ CTX}$ = 21.607; $Ct_{mean\ HIPP}$ = 22.302), *Rps29* ($Ct_{mean\ CTX}$ = 20.481; $Ct_{mean\ HIPP}$ = 22.524), *Ppia* ($Ct_{mean\ CTX}$ = 17.834; $Ct_{mean\ HIPP}$ = 19.201) and *Gapdh* ($Ct_{mean\ CTX}$ = 17.145; $Ct_{mean\ HIPP}$ = 17.385). We used the CV as an index of variability of gene expression. The genes with the highest CV were: in male *Rer1* (CV = 17.52) and *Rpl27* (CV = 32.66) in the CTX and HIPP respectively; in female, *Ppia* (CV = 21.12) and *Rpl27* (CV = 34.49) in the CTX and HIPP respectively; in both sexes group, *Ppia* (CV = 19.15) and *Rpl27* (CV = 33.74) in the CTX and HIPP respectively. The candidate gene that exhibited the lowest variability in expression levels was *Gapdh* in all analyzed groups and brain areas (male: CV_{CTX} = 12.65; CV_{HIPP} = 22.09; female: CV_{CTX} = 12.95; CV_{HIPP} = 23.85; all animals: CV_{CTX} = 13.37; CV_{HIPP} = 23.01).

We then analyzed whether development of AD-like pathology altered the expression of the candidate RGs comparing 5XFAD mice with B6SJL mice of different ages, and therefore at different stages of the disease (Fig. 2). In the CTX, *Gapdh* and *Rer1* expression was significantly lower in 5XFAD mice at 7 and 10 mo, when considering females alone or both sexes together (*Gapdh*: Female: 7 mo: $p = 0.013$; 10 mo: $p = 0.002$; All animals: 7 mo: $p = 0.016$; 10 mo: $p = 0.002$; *Rer1*: Female: 7 mo: $p = 0.055$; 10 mo: $p = 0.009$; All animals: 7 mo: $p = 0.003$; 10 mo: $p = 0.002$). Analogously, *Ppia* mRNA levels were decreased at 7 (Male: $p = 0.026$; All animals: $p = 0.025$) and 10 (irrespective of sex) mo (Male: $p = 0.002$; Female: $p = 0.005$; All animals: $p < 0.001$). At 10 mo, *Rpl27* and *Rps29*

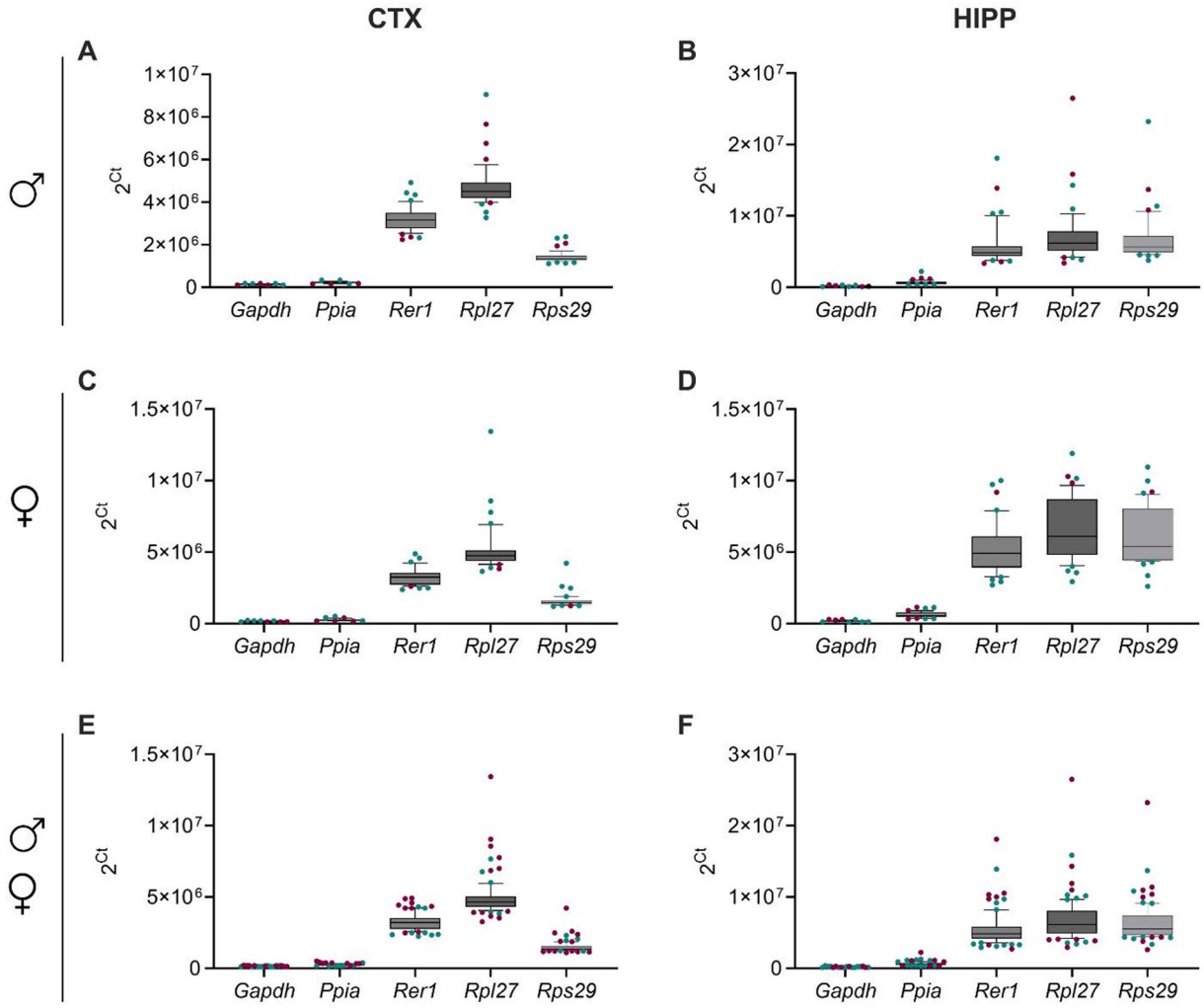

Fig. 1. Distribution of Ct values of candidate reference genes. B6SJL and 5XFAD mice were sacrificed at 2, 4, 7 and 10 mo and brains were isolated and dissected. The mRNA expression of RGs in the CTX (**A**, **C**,**E**) and HIPP (**B**, **D**,**F**) of male (**A**, **B**), female (**C**, **D**) and all (**E**, **F**) mice was determined by RT-qPCR. Box-plot graphs show averaged 2^{Ct} values of five candidate RGs. The median is represented by the line across the box and whiskers correspond to 10th and the 90th percentiles with burgundy and petrol dots representing, respectively, B6SJL and 5XFAD mice, over/under percentiles. **Abbreviations**: Ct: cycle threshold; CTX: cerebral cortex; HIPP: hippocampus; *Gapdh*: glyceraldehyde-3-phosphate dehydrogenase; *Ppia*: peptidylprolyl isomerase A; *Rer1*: retention in endoplasmic reticulum sorting receptor 1; *Rpl27*: ribosomal protein L27; *Rps29*: ribosomal protein S29.

were found significantly different with respect to B6SJL mice being increased in males ($p = 0.028$ and $p = 0.003$, respectively) and decreased in females ($p = 0.016$ and $p = 0.024$, respectively). In the HIPP, *Gapdh* was found to be decreased only at 7 mo and 10 mo in females ($p = 0.040$ and $p = 0.052$, respectively) and at 7mo when considering both sexes together ($p = 0.034$). *Rer1* expression was found to be lower in 7 mo males compared to age-matched B6SJL ($p = 0.033$) (see **Statistical report**).

Comparative analysis of candidate reference gene expression at different ages

The stability of RG expression across the different experimental conditions was analyzed using 4 different methods. Based on the stability value or SD obtained from GeNorm, NormFinder, BestKeeper and EndoGene methods, RGs were ranked from 1 (most stable) to 5 (least stable) and the geometric mean of each rank value was calculated to obtain a consensus value. The 2 genes exhibiting the lower consensus value (consensus ranks 1 and 2) were considered the most stable. Each candidate RG was analyzed irrespective of genotype/age (all animals) or considering genotype (B6SJL, 5XFAD) or age (2mo, 4mo, 7mo, 10mo) separately. Additionally, all analyses were performed in male and female mice separately as well as together (all animals) (Tables 2, 3, 4, 5, 6 and 7).

On the basis of the consensus analysis reported in Tables 2, 3, 4, 5, 6 and 7, we proceeded with the identification of the two most stable (2MS) RGs at each experimental age, and used them as internal control to evaluate the expression of all other RGs in the CTX and HIPP of 5XFAD mice compared to B6SJL. In particular, in the CTX

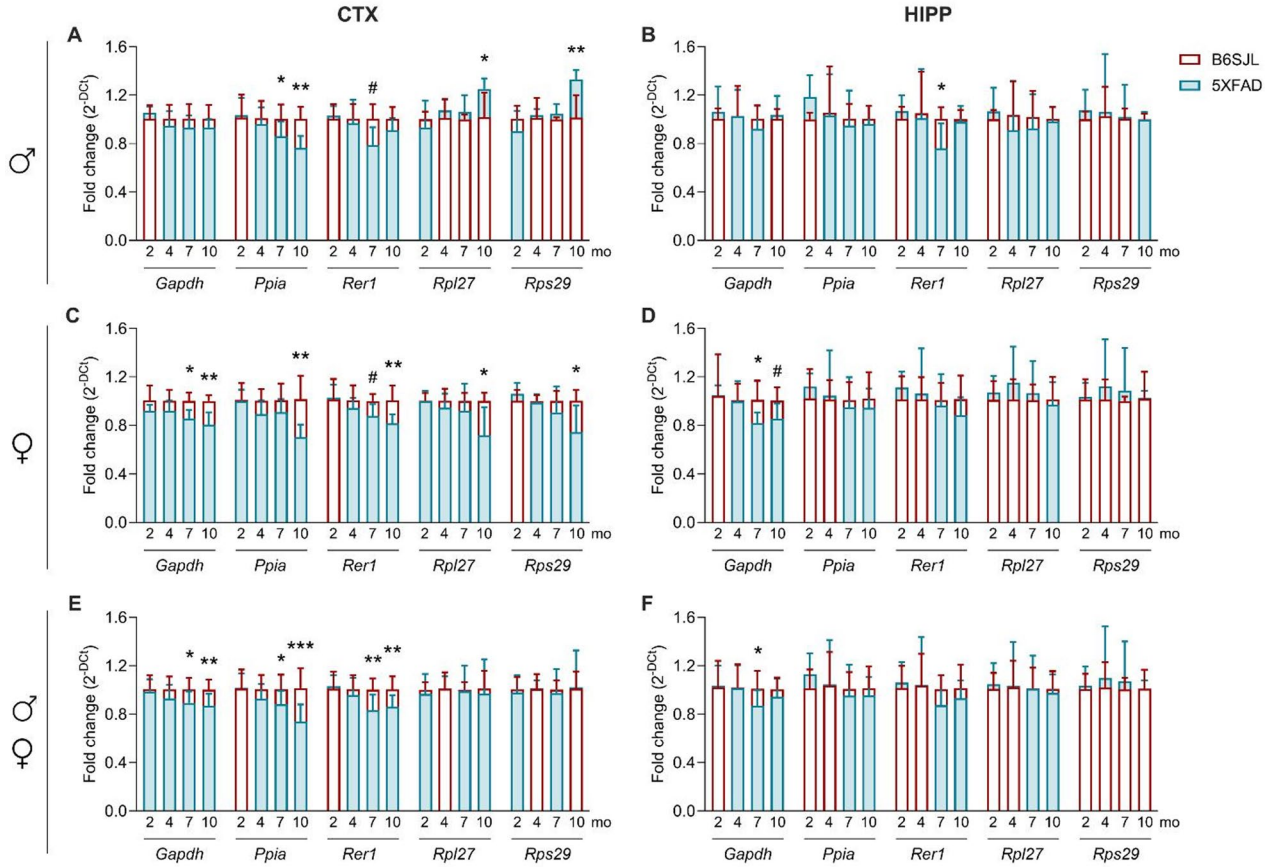

Fig. 2. Differential expression of candidate RGs in B6SJL and 5XFAD mice. The mRNA expression of candidate RGs in the CTX **(A**, **C**, **E)** and HIPP **(B**, **D**, **F)** of male **(A**, **B)**, female **(C**, **D)** mice and all animals **(E**, **F)** was determined by RT-qPCR. Graphs show averaged 2^{-DCt} values ± SD of the five candidate RGs normalized over B6SJL group at each experimental age. Burgundy and petrol histograms represent, respectively, B6SJL (2 mo: $n = 6$ M, 6 F; 4 mo: $n = 6$ M, 6 F; 7 mo: $n = 5$ M, 4 F; 10 mo: $n = 5$ M, 6 F) and 5XFAD (2 mo: $n = 6$ M, 6 F; 4 mo: $n = 6$ M, 6 F; 7 mo: $n = 6$ M, 6 F; 10 mo: $n = 6$ M, 6 F) mice. One way ANOVA was performed; # $0.10 > p > 0.05$, * $p \leq 0.05$, ** $p < 0.01$, *** $p < 0.001$ vs. B6SJL. **Abbreviations**: Ct: cycle threshold; CTX: cerebral cortex; HIPP: hippocampus; *Gapdh*: glyceraldehyde-3-phosphate dehydrogenase; *Ppia*: peptidylprolyl isomerase A; *Rer1*: retention in endoplasmic reticulum sorting receptor 1; *Rpl27*: ribosomal protein L27; *Rps29*: ribosomal protein S29; SD: standard deviation.

the 2MS RGs for each group were as follows: male: 2 mo (Fig. 3A): *Gapdh* - *Rer1*; 4 mo (Fig. 3D): *Gapdh* - *Rps29*; 7 mo (Fig. 3G): *Gapdh* - *Rps29*; 10 mo (Fig. 3J): *Gapdh* - *Rer1*. Female: 2 mo (Fig. 3B): *Ppia* - *Rpl27*; 4 mo (Fig. 3E): *Gapdh* - *Rps29*; 7 mo (Fig. 3H): *Ppia* - *Gapdh*; 10 mo (Fig. 3K): *Gapdh* - *Rer1*. All animals: 2 mo (Fig. 3C): *Gapdh* - *Rer1*; 4 mo (Fig. 3F): *Rpl27* - *Rps29*; 7 mo (Fig. 3I): *Gapdh* - *Ppia*; 10 mo (Fig. 3L): *Gapdh* - *Rer1*.

Firstly, to assess the effect of genotype on RG expression, RGs were analyzed in the CTX of experimental mice (Fig. 3).

At 2 and 4 mo, in female mice, no significant main effect of genotype or genotype*RG interaction (Genotype: $F(1,10) = 0.014$; $p = 0.907$; RGs: $F(2,20) = 2.554$; $p = 0.103$; Genotype*RGs: $F(2,20) = 2.355$; $p = 0.121$) was observed for *Gapdh* in 5XFAD mice compared to controls (Fig. 3B).

At 7 mo, RG expression was significantly influenced by genotype in male group as evidenced by a significant genotype*RG interaction (Genotype: $F(1,9) = 4.978$; $p = 0.053$; RGs: $F(2,18) = 8.498$; $p = 0.003$; Genotype*RGs: $F(2,19) = 9.059$; $p = 0.003$). Specifically, *Ppia* and *Rer1* were significantly downregulated in 5XFAD mice compared to controls, while *Rpl27* expression remained unaffected (Fig. 3G). In all animal groups, RG expression was not affected by genotype with no statistically significant effects detected (Genotype: $F(1,19) = 1.233$; $p = 0.281$; RGs: $F(2,38) = 2.738$; $p = 0.077$; Genotype*RGs: $F(2,38) = 2.702$; $p = 0.080$). No significant changes were observed in the CTX of female and all animal groups at 4 or 7 mo.

At 10 mo, RG expression continued to be significantly influenced by genotype in male group (Genotype: $F(1,10) = 4.388$, $p = 0.063$; RGs: $F(2,20) = 33.729$, $p < 0.001$; Genotype*RGs: $F(2,20) = 29614$, $p < 0.001$); *Ppia* remained downregulated in 5XFAD mice, while *Rpl27* and *Rps29* were significantly upregulated (Fig. 3J). In female mice, no statistically significant effect was observed (Genotype: $F(1,10) = 1.573$; $p = 0.238$; RGs: $F(2,20) = 0.127$; $p = 0.882$; Genotype*RGs: $F(2,20) = 0.197$; $p = 0.823$) (Fig. 3K). In all animal groups, a significant genotype*RG interaction was observed, with *Ppia* expression being downregulated in 5XFAD mice (Fig. 3L)

CTX	MALE		Normfinder		GeNorm		BestKeeper		EndoGene analyzer		CONSENSUS	
			stability value	rank	stability value	rank	SD	rank	SD	rank	rank geom mean	rank
ALL ANIMALS (different genotype/age)	all animals	***Gapdh***	0.052	1	0.176	3	0.145	1	0.180	1	1.316	1
		Ppia	0.068	2	0.176	2	0.194	4	0.250	3	2.632	2
		Rer1	0.075	3	0.175	1	0.213	5	0.260	4	2.783	3
		Rpl27	0.076	4	0.255	5	0.173	3	0.260	4	3.936	5
		Rps29	0.083	5	0.248	4	0.169	2	0.240	2	2.991	4
SINGLE GENOTYPE GROUP (different ages)	B6SJL	***Gapdh***	0.037	4	0.215	5	0.156	1	0.190	1	2.115	2
		Ppia	0.025	1	0.194	3	0.163	2	0.210	2	1.861	1
		Rer1	0.033	2	0.212	4	0.188	4	0.230	3	3.130	4
		Rpl27	0.034	3	0.164	2	0.181	3	0.240	4	2.913	3
		Rps29	0.037	5	0.170	1	0.196	5	0.250	5	3.344	5
	5XFAD	***Gapdh***	0.048	1	0.167	2	0.137	1	0.180	1	1.189	1
		Ppia	0.080	2	0.170	3	0.213	4	0.270	3	2.913	3
		Rer1	0.099	4	0.164	1	0.224	5	0.270	3	2.783	2
		Rpl27	0.089	3	0.270	5	0.161	3	0.270	3	3.409	5
		Rps29	0.100	5	0.256	4	0.138	2	0.220	2	2.991	4
SINGLE AGE GROUP (different genotype)	2 mo	***Gapdh***	0.036	2	0.140	2	0.096	1	0.130	1	1.414	1*
		Ppia	0.047	4	0.146	3	0.167	5	0.220	3	3.663	3
		Rer1	0.035	1	0.130	1	0.103	2	0.140	2	1.414	1*
		Rpl27	0.053	5	0.239	5	0.163	4	0.290	5	4.729	4
		Rps29	0.043	3	0.214	4	0.160	3	0.250	4	3.464	2
	4 mo	***Gapdh***	0.027	2	0.191	4	0.126	2	0.180	1	2.000	1*
		Ppia	0.012	1	0.178	3	0.155	4	0.200	3	2.449	3
		Rer1	0.045	5	0.209	5	0.182	5	0.240	4	4.729	4
		Rpl27	0.031	3	0.151	1	0.133	3	0.190	2	2.060	2
		Rps29	0.044	4	0.159	2	0.126	1	0.190	2	2.000	1*
	7 mo	***Gapdh***	0.044	1	0.142	3	0.146	3	0.170	3	2.280	2
		Ppia	0.063	2	0.172	4	0.155	4	0.210	4	3.364	4
		Rer1	0.099	5	0.200	5	0.242	5	0.290	5	5.000	5
		Rpl27	0.082	4	0.124	2	0.094	2	0.140	2	2.378	3
		Rps29	0.073	3	0.118	1	0.064	1	0.090	1	1.316	1
	10 mo	***Gapdh***	0.078	1	0.289	4	0.103	1	0.140	1	1.414	1
		Ppia	0.136	4	0.310	5	0.212	3	0.260	3	3.663	4
		Rer1	0.092	2	0.282	3	0.132	2	0.160	2	2.213	2
		Rpl27	0.120	3	0.238	1	0.213	4	0.270	4	2.632	3
		Rps29	0.142	5	0.241	2	0.226	5	0.290	5	3.976	5

Table 2. Analysis and ranking of the stability of five candidate RGs in the CTX of male animals. The results of the analysis of RG stability with four different methods, namely NormFinder, GeNorm, Bestkeeper and endogene are shown. For each method, RGs have been ranked from 1 (more stable) to 5 (least stable) based on their stability. For each RG, a consensus value was obtained by calculating the geometric mean of the ranking of the 4 methods. The 2 RGs with the lowest consensus value were considered the most stable (consensus ranking 1 and 2). **Abbreviations**: CTX: cerebral cortex; *Gapdh*: glyceraldehyde-3-phosphate dehydrogenase; *Ppia*: peptidylprolyl isomerase A; *Rer1*: retention in Endoplasmic reticulum sorting receptor 1; *Rpl27*: ribosomal protein L27; *Rps29*: ribosomal protein S29; SD: standard deviation.

(10 mo: Genotype: $F(1,22) = 0.242$; $p = 0.628$; RGs: $F(2,44) = 9.342$; $p < 0.001$; Genotype*RGs: $F(2,44) = 9.214$; $p < 0.001$).

The same analysis was performed in the HIPP (Fig. 4); the 2MS RGs for each group and time point were as follows: Male: 2 mo (Fig. 4A): *Gapdh* - *Ppia*; 4 mo (Fig. 4D): *Gapdh* - *Rps29*; 7 mo (Fig. 4G): *Gapdh* - *Ppia*; 10 mo (Fig. 4J): *Rps29* - *Rer1*. Female: 2 mo (Fig. 4B): *Rpl27* - *Rps29*; 4 mo (Fig. 4E): *Gapdh* - *Rps29*; 7 mo (Fig. 4H): *Rpl27* - *Rps29*; 10 mo (Fig. 4K): *Rpl27* - *Rps29*. All animals: 2 mo (Fig. 4C): *Rpl27* - *Rps29*; 4 mo (Fig. 4F): *Gapdh* - *Rps29*; 7 mo (Fig. 4I): *Gapdh* - *Ppia*; 10 mo (Fig. 4L): *Rpl27* - *Rps29*.

In the HIPP, at 2 and 4 mo no significant effect was observed in 5XFAD mice (Fig. 4A-F).

At 7 mo, a trend for a significant reduction was observed for *Rer1* expression in 5XFAD male mice (Fig. 4G) (Male: Genotype: $F(1,8) = 0.460$, $p = 0.517$; RGs: $F(2,16) = 4.130$, $p = 0.036$; Genotype*RGs: $F(2,16) = 4.551$, $p = 0.027$); in female mice, a trend for a significant reduction was observed for *Gapdh* in 5XFAD mice (Fig. 4H) (Genotype: $F(1,9) = 5.166$, $p = 0.049$; RGs: $F(2,18) = 0.956$, $p = 0.400$; Genotype*RGs: $F(2,18) = 0.948$, $p = 0.406$).

CTX	FEMALE		Normfinder		GeNorm		BestKeeper		EndoGene analyzer		CONSENSUS	
			stability value	rank	stability value	rank	SD	rank	SD	rank	rank geom mean	rank
ALL ANIMALS (different genotype/age)	all animals	***Gapdh***	0.060	4	0.193	2	0.144	1	0.190	1	1.682	1
		Ppia	0.055	1	0.199	3	0.265	5	0.350	5	2.943	4
		Rer1	0.059	3	0.177	1	0.209	4	0.260	2	2.213	2
		Rpl27	0.058	2	0.257	4	0.205	2	0.330	4	2.828	3
		Rps29	0.066	5	0.263	5	0.206	3	0.320	3	3.873	5
SINGLE GENOTYPE GROUP (different ages)	B6SJL	***Gapdh***	0.056	2	0.159	3	0.126	3	0.160	3	2.711	3
		Ppia	0.051	1	0.186	5	0.186	4	0.270	5	3.162	4
		Rer1	0.061	4	0.178	4	0.199	5	0.240	4	4.229	5
		Rpl27	0.057	3	0.148	1	0.096	1	0.120	1	1.316	1
		Rps29	0.061	5	0.149	2	0.113	2	0.130	2	2.515	2
	5XFAD	***Gapdh***	0.070	3	0.208	2	0.130	1	0.180	1	1.565	1
		Ppia	0.074	4	0.217	3	0.310	5	0.390	3	3.663	4
		Rer1	0.063	2	0.192	1	0.210	2	0.270	2	1.682	2
		Rpl27	0.062	1	0.303	4	0.295	4	0.420	4	2.828	3
		Rps29	0.077	5	0.316	5	0.295	3	0.420	4	4.162	5
SINGLE AGE GROUP (different genotype)	2 mo	***Gapdh***	0.042	4	0.124	3	0.121	3	0.150	3	3.224	3
		Ppia	0.024	1	0.111	1	0.138	4	0.180	4	2.000	4
		Rer1	0.037	3	0.120	2	0.158	5	0.210	5	3.500	5
		Rpl27	0.035	2	0.143	4	0.089	1	0.110	1	1.682	1
		Rps29	0.045	5	0.156	5	0.103	2	0.130	2	3.162	2
	4 mo	***Gapdh***	0.014	1	0.143	3	0.106	2	0.150	2	1.861	2
		Ppia	0.031	3	0.159	4	0.125	5	0.180	4	3.936	4
		Rer1	0.038	4	0.171	5	0.111	3	0.150	2	3.310	3*
		Rpl27	0.041	5	0.136	2	0.125	4	0.160	3	3.310	3*
		Rps29	0.020	2	0.132	1	0.066	1	0.090	1	1.189	1
	7 mo	***Gapdh***	0.013	1	0.112	1	0.128	1	0.160	1	1.000	1
		Ppia	0.034	2	0.113	2	0.139	3	0.190	2	2.213	2*
		Rer1	0.039	4	0.114	3	0.130	2	0.160	1	2.213	2*
		Rpl27	0.043	5	0.228	5	0.200	4	0.300	3	4.162	4
		Rps29	0.037	3	0.213	4	0.201	5	0.300	3	3.663	3
	10 mo	***Gapdh***	0.042	4	0.182	2	0.171	1	0.210	1	1.682	2
		Ppia	0.041	3	0.194	3	0.307	4	0.370	3	3.224	4
		Rer1	0.028	1	0.166	1	0.185	2	0.220	2	1.414	1
		Rpl27	0.045	5	0.327	5	0.351	5	0.460	5	5.000	5
		Rps29	0.038	2	0.308	4	0.288	3	0.450	4	3.130	3

Table 3. Analysis and ranking of the stability of five candidate RGs in the CTX of female animals. The results of the analysis of RG stability with four different methods, namely NormFinder, GeNorm, Bestkeeper and Endogene are shown. For each method, RGs have been ranked from 1 (more stable) to 5 (least stable) based on their stability. For each RG, a consensus value was obtained by calculating the geometric mean of the ranking of the 4 methods. The 2 RGs with the lowest consensus value were considered the most stable (consensus ranking 1 and 2). **Abbreviations**: CTX: cerebral cortex; *Gapdh*: glyceraldehyde-3-phosphate dehydrogenase; *Ppia*: peptidylprolyl isomerase A; *Rer1*: retention in Endoplasmic reticulum sorting receptor 1; *Rpl27*: ribosomal protein L27; *Rps29*: ribosomal protein S29; SD: standard deviation.

At the same age, *Rps29* expression was significantly increased in 5XFAD mice in all animal groups (Fig. 4I) (Genotype: $F(1,19) = 1.400$, $p = 0.251$; RGs: $F(2,38) = 6.059$, $p = 0.005$; Genotype*RGs: $F(2,38) = 6.501$, $p = 0.004$).

At 10 mo, *Rer1* showed a trend towards a significantly reduced expression in 5XFAD female mice (Fig. 5K) (Genotype: $F(1,10) = 5.315$, $p = 0.044$; RGs: $F(2,20) = 0.402$, $p = 0.674$; Genotype*RGs: $F(2,20) = 0.537$, $p = 0.593$). No significant differences were observed in other groups at this time point.

Overall, these findings demonstrated that RG expression is variably affected by genotype, with more prominent changes emerging at later stages (7, 10 mo), particularly in male 5XFAD mice, and in CTX.

Reference gene validation

In order to demonstrate the impact of RG selection on normalization of RT-qPCR data, we selected four target genes (TGs), namely *Hexb*, *Lpl4*, *Cx3cr1* and *Cx3cl1*, on the basis of previous RNA sequencing analysis demonstrating their significant alterations in the same experimental set-up (unpublished data), and assessed

CTX			Normfinder		GeNorm		BestKeeper		EndoGene analyzer		CONSENSUS	
			stability value	rank	stability value	rank	SD	rank	SD	rank	rank geom mean	rank
ALL ANIMALS (different genotype/age)	all animals	***Gapdh***	0.052	4	0.360	4	0.710	1	0.380	1	2.000	2
		Ppia	0.044	2	0.263	1	0.860	4	0.590	3	2.213	3
		Rer1	0.061	5	0.270	2	0.910	5	0.580	2	3.162	5
		Rpl27	0.045	3	0.263	1	0.840	3	0.640	4	2.449	4
		Rps29	0.038	1	0.328	3	0.790	2	0.580	2	1.861	1
SINGLE GENOTYPE GROUP (different ages)	B6SJL	***Gapdh***	0.058	3	0.311	4	0.250	1	0.350	1	1.861	1
		Ppia	0.060	4	0.268	2	0.390	5	0.480	3	3.310	4
		Rer1	0.070	5	0.277	3	0.340	3	0.480	3	3.409	5
		Rpl27	0.052	2	0.267	1	0.380	4	0.480	3	2.213	3
		Rps29	0.043	1	0.379	5	0.320	2	0.410	2	2.115	2
	5XFAD	***Gapdh***	0.057	5	0.304	5	0.310	1	0.410	1	2.236	2
		Ppia	0.031	1	0.179	3	0.460	2	0.700	3	2.060	1
		Rer1	0.055	4	0.219	4	0.480	3	0.660	2	3.130	4
		Rpl27	0.050	3	0.166	2	0.560	5	0.770	5	3.500	5
		Rps29	0.032	2	0.152	1	0.520	4	0.730	4	2.378	3
SINGLE AGE GROUP (different genotype)	2 mo	***Gapdh***	0.042	5	0.212	5	0.240	1	0.330	1	2.236	1
		Ppia	0.009	1	0.100	3	0.340	3	0.610	3	2.280	2
		Rer1	0.026	4	0.119	4	0.330	2	0.590	2	2.828	5
		Rpl27	0.023	3	0.092	2	0.340	3	0.610	3	2.711	4
		Rps29	0.013	2	0.086	1	0.390	4	0.620	4	2.378	3
	4 mo	***Gapdh***	0.083	5	0.382	5	0.280	1	0.340	1	2.236	2
		Ppia	0.051	4	0.283	4	0.420	3	0.560	2	3.130	4
		Rer1	0.027	2	0.235	2	0.460	4	0.570	3	2.632	3
		Rpl27	0.046	3	0.252	3	0.560	5	0.610	5	3.873	5
		Rps29	0.022	1	0.229	1	0.350	2	0.580	4	1.682	1
	7 mo	***Gapdh***	0.048	2	0.193	2	0.160	1	0.210	1	1.414	1
		Ppia	0.044	1	0.183	1	0.210	2	0.280	3	1.565	2
		Rer1	0.090	5	0.235	4	0.260	3	0.340	4	3.936	5
		Rpl27	0.052	3	0.206	3	0.290	4	0.360	5	3.663	4
		Rps29	0.062	4	0.416	5	0.160	1	0.240	2	2.515	3
	10 mo	***Gapdh***	0.037	4	0.182	4	0.140	5	0.170	4	4.229	4
		Ppia	0.038	5	0.193	5	0.130	4	0.200	5	4.729	5
		Rer1	0.030	2	0.155	3	0.100	2	0.140	2	2.213	2
		Rpl27	0.036	3	0.147	2	0.120	3	0.150	3	2.711	3
		Rps29	0.014	1	0.143	1	0.060	1	0.080	1	1.000	1

Table 4. Analysis and ranking of the stability of five candidate RGs in the CTX of all animals. The results of the analysis of RG stability with four different methods, namely NormFinder, GeNorm, Bestkeeper and Endogene are shown. For each method, RGs have been ranked from 1 (more stable) to 5 (least stable) based on their stability. For each RG, a consensus value was obtained by calculating the geometric mean of the ranking of the 4 methods. The 2 RGs with the lowest consensus value were considered the most stable (consensus ranking 1 and 2). **Abbreviations**: CTX: cerebral cortex; *Gapdh*: glyceraldehyde-3-phosphate dehydrogenase; *Ppia*: peptidylprolyl isomerase A; *Rer1*: retention in Endoplasmic reticulum sorting receptor 1; *Rpl27*: ribosomal protein L27; *Rps29*: ribosomal protein S29; SD: standard deviation.

their expression in the CTX (Fig. 5) and HIPP (Fig. 6) of age-matched B6SJL and 5XFAD mice. Subsequently, expression levels of the TGs were normalized and compared using 3 calibrators: the 2MS RGs, the LS RG or A RGs, identified in our previous analysis (see Tables 2, 3, 4, 5, 6 and 7).

Cerebral cortex

Hexb expression

At 2 mo, *Hexb* expression did not differ significantly between B6SJL and 5XFAD in both male and female mice, with similar values across all datasets (Male: 2MS, LS, A RGs: $p > 0.5$; Female: 2MS, LS, or A RGs: $p > 0.6$). By 4 mo, a clear upregulation was detected in 5XFAD mice compared to controls across all datasets in both male (*Mean*: 2MS: 1.492, $p < 0.001$; LS: 1.582, $p = 0.017$; A: 1.495, $p < 0.001$) and female (*Mean*: 2MS: 1.595, $p = 0.002$; LS: 1.735, $p = 0.007$; A: 1.036, $p = 0.003$) mice, though, normalization with the LS RG led to a slightly higher variability (Male: SD = 0.463; Female: SD = 0.439). This upregulation became more pronounced at 7 mo, when

HIPP	MALE		Normfinder		GeNorm		BestKeeper		EndoGene analyzer		CONSENSUS	
			stability value	rank	stability value	rank	SD	rank	SD	rank	rank geom mean	rank
ALL ANIMALS (different genotype/age)	all animals	***Gapdh***	0.052	4	0.360	4	0.710	1	0.380	1	2.000	2
		Ppia	0.044	2	0.263	1	0.860	4	0.590	3	2.213	3
		Rer1	0.061	5	0.270	2	0.910	5	0.580	2	3.162	5
		Rpl27	0.045	3	0.263	1	0.840	3	0.640	4	2.449	4
		Rps29	0.038	1	0.328	3	0.790	2	0.580	2	1.861	1
SINGLE GENOTYPE GROUP (different ages)	B6SJL	***Gapdh***	0.058	3	0.311	4	0.250	1	0.350	1	1.861	1
		Ppia	0.060	4	0.268	2	0.390	5	0.480	3	3.310	4
		Rer1	0.070	5	0.277	3	0.340	3	0.480	3	3.409	5
		Rpl27	0.052	2	0.267	1	0.380	4	0.480	3	2.213	3
		Rps29	0.043	1	0.379	5	0.320	2	0.410	2	2.115	2
	5XFAD	***Gapdh***	0.057	5	0.304	5	0.310	1	0.410	1	2.236	2
		Ppia	0.031	1	0.179	3	0.460	2	0.700	3	2.060	1
		Rer1	0.055	4	0.219	4	0.480	3	0.660	2	3.130	4
		Rpl27	0.050	3	0.166	2	0.560	5	0.770	5	3.500	5
		Rps29	0.032	2	0.152	1	0.520	4	0.730	4	2.378	3
SINGLE AGE GROUP (different genotype)	2 mo	***Gapdh***	0.042	5	0.212	5	0.240	1	0.330	1	2.236	1
		Ppia	0.009	1	0.100	3	0.340	3	0.610	3	2.280	2
		Rer1	0.026	4	0.119	4	0.330	2	0.590	2	2.828	5
		Rpl27	0.023	3	0.092	2	0.340	3	0.610	3	2.711	4
		Rps29	0.013	2	0.086	1	0.390	4	0.620	4	2.378	3
	4 mo	***Gapdh***	0.083	5	0.382	5	0.280	1	0.340	1	2.236	2
		Ppia	0.051	4	0.283	4	0.420	3	0.560	2	3.130	4
		Rer1	0.027	2	0.235	2	0.460	4	0.570	3	2.632	3
		Rpl27	0.046	3	0.252	3	0.560	5	0.610	5	3.873	5
		Rps29	0.022	1	0.229	1	0.350	2	0.580	4	1.682	1
	7 mo	***Gapdh***	0.048	2	0.193	2	0.160	1	0.210	1	1.414	1
		Ppia	0.044	1	0.183	1	0.210	2	0.280	3	1.565	2
		Rer1	0.090	5	0.235	4	0.260	3	0.340	4	3.936	5
		Rpl27	0.052	3	0.206	3	0.290	4	0.360	5	3.663	4
		Rps29	0.062	4	0.416	5	0.160	1	0.240	2	2.515	3
	10 mo	***Gapdh***	0.037	4	0.182	4	0.140	5	0.170	4	4.229	4
		Ppia	0.038	5	0.193	5	0.130	4	0.200	5	4.729	5
		Rer1	0.030	2	0.155	3	0.100	2	0.140	2	2.213	2
		Rpl27	0.036	3	0.147	2	0.120	3	0.150	3	2.711	3
		Rps29	0.014	1	0.143	1	0.060	1	0.080	1	1.000	1

Table 5. Analysis and ranking of the stability of five candidate RGs in the HIPP of male animals. The results of the analysis of RG stability with four different methods, namely NormFinder, GeNorm, Bestkeeper and Endogene are shown. For each method, RGs have been ranked from 1 (more stable) to 5 (least stable) based on their stability. For each RG, a consensus value was obtained by calculating the geometric mean of the ranking of the 4 methods. The 2 RGs with the lowest consensus value were considered the most stable (consensus ranking 1 and 2). **Abbreviations**: HIPP: hippocampus; *Gapdh*: glyceraldehyde-3-phosphate dehydrogenase; *Ppia*: peptidylprolyl isomerase A; *Rer1*: retention in Endoplasmic reticulum sorting receptor 1; *Rpl27*: ribosomal protein L27; *Rps29*: ribosomal protein S29; SD: standard deviation.

expression increased more than two fold in 5XFAD mice in both male (*Mean*: 2MS: 2.373; LS: 3.051; A: 2.530; all $p < 0.001$) and female (*Mean* 2MS: 3.010; $p = 0.002$; LS: 2.887, $p < 0.001$; A: 2.950, $p < 0.001$) mice reflecting substantial enzymatic activation associated with disease progression. In the CTX of male mice, elevated expression persisted at 10 mo, in all datasets (*Mean*: 2MS: 2.774; LS: 1.903; A: 2.506; all $p < 0.001$); 2MS- and A-normalized groups showed higher upregulation than LS-normalized samples. In the female group, at 10 mo, *Hexb* expression remained significantly elevated at the same levels irrespective of the normalization (*Mean*: 2MS: 2.543, $p < 0.001$; LS: 2.924, $p < 0.001$; A: 2.709, $p < 0.001$).

Lpl4 expression

No significant changes in *Lpl4* expression were observed in 2 or 4 mo female and 2 mo male 5XFAD mice ($p > 0.5$). By 4 mo in males, *Lpl4* expression showed a significant increase in 5XFAD mice, regardless of RG used for normalization (*Mean*: 2MS: 1.263; LS: 1.322; A: 1.260). This upregulation became more pronounced by 7 mo

HIPP	FEMALE		Normfinder		GeNorm		BestKeeper		EndoGene analyzer		CONSENSUS	
			stability value	rank	stability value	rank	SD	rank	SD	rank	rank geom mean	rank
ALL ANIMALS (different genotype/age)	all animals	***Gapdh***	0.062	3	0.248	4	0.420	1	0.350	1	1.861	2
		Ppia	0.041	2	0.297	5	0.540	4	0.480	3	3.310	5
		Rer1	0.038	1	0.185	3	0.520	3	0.460	2	2.060	3
		Rpl27	0.038	1	0.180	2	0.560	5	0.500	4	2.515	4
		Rps29	0.038	1	0.173	1	0.510	2	0.460	2	1.414	1
SINGLE GENOTYPE GROUP (different ages)	B6SJL	***Gapdh***	0.054	5	0.233	3	0.460	2	0.410	1	2.340	2
		Ppia	0.037	4	0.323	4	0.530	4	0.500	4	4.000	5
		Rer1	0.036	3	0.174	2	0.490	3	0.480	3	2.711	4
		Rpl27	0.033	2	0.169	1	0.540	5	0.520	5	2.659	3
		Rps29	0.027	1	0.169	1	0.440	1	0.440	2	1.189	1
	5XFAD	***Gapdh***	0.053	4	0.244	5	0.200	1	0.250	1	2.115	2
		Ppia	0.037	3	0.170	1	0.390	3	0.470	3	2.280	3
		Rer1	0.033	2	0.173	2	0.320	2	0.450	2	2.000	1
		Rpl27	0.037	3	0.192	4	0.400	4	0.500	5	3.936	5
		Rps29	0.029	1	0.174	3	0.390	3	0.490	4	2.449	4
SINGLE AGE GROUP (different genotype)	2 mo	***Gapdh***	0.039	5	0.211	4	0.470	5	0.300	5	4.729	5
		Ppia	0.028	2	0.352	5	0.450	4	0.250	4	3.557	4
		Rer1	0.033	4	0.152	2	0.390	3	0.230	3	2.913	3
		Rpl27	0.025	1	0.133	1	0.330	2	0.200	2	1.414	1
		Rps29	0.030	3	0.160	3	0.270	1	0.190	1	1.732	2
	4 mo	***Gapdh***	0.060	5	0.217	5	0.170	1	0.220	1	2.236	2
		Ppia	0.022	3	0.113	2	0.330	3	0.400	4	2.913	4
		Rer1	0.025	4	0.116	3	0.340	4	0.410	5	3.936	5
		Rpl27	0.015	2	0.158	4	0.260	2	0.320	2	2.378	3
		Rps29	0.008	1	0.110	1	0.330	3	0.380	3	1.732	1
	7 mo	***Gapdh***	0.100	5	0.228	5	0.190	3	0.240	1	2.943	4
		Ppia	0.040	2	0.181	4	0.230	5	0.280	3	3.310	5
		Rer1	0.038	1	0.173	3	0.210	4	0.270	2	2.213	3
		Rpl27	0.070	3	0.166	2	0.180	2	0.240	1	1.861	2
		Rps29	0.077	4	0.162	1	0.140	1	0.270	2	1.682	1
	10 mo	***Gapdh***	0.055	5	0.209	5	0.160	2	0.210	1	2.659	3
		Ppia	0.029	1	0.165	2	0.210	3	0.270	3	2.060	2
		Rer1	0.042	3	0.183	4	0.230	4	0.270	3	3.464	4
		Rpl27	0.033	2	0.162	1	0.210	3	0.250	2	1.861	1*
		Rps29	0.047	4	0.169	3	0.150	1	0.210	1	1.861	1*

Table 6. Analysis and ranking of the stability of five candidate RGs in the HIPP of female animals. The results of the analysis of RG stability with four different methods, namely NormFinder, GeNorm, Bestkeeper and Endogene are shown. For each method, RGs have been ranked from 1 (more stable) to 5 (least stable) based on their stability. For each RG, a consensus value was obtained by calculating the geometric mean of the ranking of the 4 methods. The 2 RGs with the lowest consensus value were considered the most stable (consensus ranking 1 and 2). **Abbreviations**: HIPP: hippocampus; *Gapdh*: glyceraldehyde-3-phosphate dehydrogenase; *Ppia*: peptidylprolyl isomerase A; *Rer1*: retention in Endoplasmic reticulum sorting receptor 1; *Rpl27*: ribosomal protein L27; *Rps29*: ribosomal protein S29; SD: standard deviation.

in both sexes, with males showing increases across datasets (*Mean*: 2MS: 1.638; LS: 2.112; A: 1.748) and females displaying a comparable rise (2MS: 1.679; LS: 1.600; A: 1.646). Notably, the LS dataset showed slightly greater variability in the cortex at 7 mo (SD = 0.243). At 10 mo, *Lpl4* expression declined toward control levels in both male (*Mean*: 2MS: 1.343; LS: 0.929; A: 1.213), and female (*Mean*: 2MS: 1.273; LS: 1.440; A: 1.347) mice. Despite this reduction, significant differences were still detected in females across all datasets (*Mean*: 2MS: $p = 0.041$; LS: $p = 0.001$; A: $p = 0.003$). Variability was again higher in the LS dataset at 10 mo (SD = 0.703).

Cx3cr1 expression

At 2 mo, *Cx3cr1* expression remained stable and comparable between genotypes in both male ($p > 0.1$) and female ($p > 0.4$) groups. By 4 mo, a significant increase in expression was observed exclusively in female 5XFAD mice across all datasets (*Mean*: 2MS: $p < 0.001$; LS: $p < 0.001$; A: $p < 0.001$), while no significant changes were detected in males (*Mean*: $p > 0.1$ for all datasets). From 7 mo onward, Cx3cr1 expression showed a dramatic

HIPP			Normfinder		GeNorm		BestKeeper		EndoGene analyzer		CONSENSUS	
			stability value	rank	stability value	rank	SD	rank	SD	rank	rank geom mean	rank
ALL ANIMALS (different genotype/age)	all animals	***Gapdh***	0.044	5	0.334	5	0.550	1	0.360	1	2.236	3
		Ppia	0.034	3	0.306	4	0.680	3	0.540	3	3.224	5
		Rer1	0.039	4	0.273	2	0.710	4	0.520	2	2.828	4
		Rpl27	0.033	2	0.266	1	0.680	3	0.570	4	2.213	2
		Rps29	0.030	1	0.285	3	0.630	2	0.520	2	1.861	1
SINGLE GENOTYPE GROUP (different ages)	B6SJL	***Gapdh***	0.041	5	0.287	3	0.350	1	0.380	1	1.968	1
		Ppia	0.038	4	0.334	4	0.460	4	0.490	4	4.000	5
		Rer1	0.036	3	0.269	1	0.420	3	0.480	3	2.280	3
		Rpl27	0.034	2	0.275	2	0.460	4	0.490	4	2.828	4
		Rps29	0.023	1	0.363	5	0.380	2	0.420	2	2.115	2
	5XFAD	***Gapdh***	0.043	5	0.310	5	0.250	1	0.340	1	2.236	2
		Ppia	0.032	2	0.187	3	0.430	3	0.590	3	2.711	3
		Rer1	0.036	4	0.208	4	0.400	2	0.560	2	2.828	4
		Rpl27	0.035	3	0.179	2	0.480	5	0.650	5	3.500	5
		Rps29	0.024	1	0.167	1	0.460	4	0.620	4	2.000	1
SINGLE AGE GROUP (different genotype)	2 mo	***Gapdh***	0.027	4	0.232	4	0.360	3	0.320	1	2.632	3*
		Ppia	0.020	3	0.310	5	0.410	5	0.460	4	4.162	4
		Rer1	0.019	2	0.154	3	0.400	4	0.440	2	2.632	3*
		Rpl27	0.017	1	0.132	1	0.350	2	0.440	2	1.414	1
		Rps29	0.017	1	0.143	2	0.330	1	0.450	3	1.565	2
	4 mo	***Gapdh***	0.046	5	0.309	5	0.230	1	0.290	1	2.236	2
		Ppia	0.024	3	0.205	3	0.370	3	0.500	3	3.000	5
		Rer1	0.015	2	0.185	1	0.420	4	0.510	4	2.378	3
		Rpl27	0.027	4	0.227	4	0.350	2	0.490	2	2.828	4
		Rps29	0.011	1	0.191	2	0.370	3	0.500	3	2.060	1
	7 mo	***Gapdh***	0.061	5	0.231	4	0.170	1	0.230	1	2.115	2
		Ppia	0.022	1	0.205	1	0.230	3	0.280	2	1.565	1
		Rer1	0.047	3	0.211	3	0.230	3	0.310	3	3.000	5
		Rpl27	0.039	2	0.207	2	0.230	3	0.310	3	2.449	3
		Rps29	0.055	4	0.344	5	0.190	2	0.280	2	2.991	4
	10 mo	***Gapdh***	0.032	5	0.211	5	0.150	2	0.190	2	3.162	4
		Ppia	0.017	2	0.178	3	0.170	4	0.240	4	3.130	3
		Rer1	0.023	4	0.191	4	0.200	5	0.240	4	4.229	5
		Rpl27	0.018	3	0.170	2	0.160	3	0.200	3	2.711	2
		Rps29	0.015	1	0.162	1	0.120	1	0.160	1	1.000	1

Table 7. Ranking of the stability of five candidate RGs in the HIPP of all animals. The results of the analysis of RG stability with four different methods, namely NormFinder, GeNorm, Bestkeeper and Endogene are shown. For each method, RGs have been ranked from 1 (more stable) to 5 (least stable) based on their stability. For each RG, a consensus value was obtained by calculating the geometric mean of the ranking of the 4 methods. The 2 RGs with the lowest consensus value were considered the most stable (consensus ranking 1 and 2). **Abbreviations**: HIPP: hippocampus; *Gapdh*: glyceraldehyde-3-phosphate dehydrogenase; *Ppia*: peptidylprolyl isomerase A; *Rer1*: retention in Endoplasmic reticulum sorting receptor 1; *Rpl27*: ribosomal protein L27; *Rps29*: ribosomal protein S29; SD: standard deviation.

increase in 5XFAD mice of both sexes. In males, expression levels nearly doubled compared to controls (*Mean*: 2MS: 1.855; LS: 2.370; A: 1.974; $p < 0.001$); in females, expression nearly tripled (*Mean*: 2MS: 2.981, $p < 0.001$; LS: 2.986, $p = 0.003$; A: 2.986, $p < 0.001$). At 10 mo, *Cx3cr1* remained highly elevated in 5XFAD mice. In males, expression was significantly increased (*Mean*: 2MS: 1.884, $p < 0.001$; LS: 1.300, $0 = 0.072$; A: 1.708, $p = 0.002$), although variability was greater in the LS-normalized dataset. In females, expression continued to show robust elevation (*Mean*: 2MS: 2.758, $p < 0.001$; LS: 3.470, $p = 0.017$; A: 3.029, $p < 0.001$) with the LS dataset again displaying the highest standard deviation.

Cx3cl1 expression

Cortical *Cx3cl1* expression was unchanged in both male ($p > 0.1$) and female ($p > 0.6$) groups at 2 and 4 mo. At 7 mo, *Cx3cl1* was significantly downregulated in male and female 5XFAD mice across most datasets. In males, expression was reduced in the 2MS (*Mean*: 0.747, $p < 0.001$), and A (*Mean*: 0.794, $p < 0.001$) RGs datasets, though

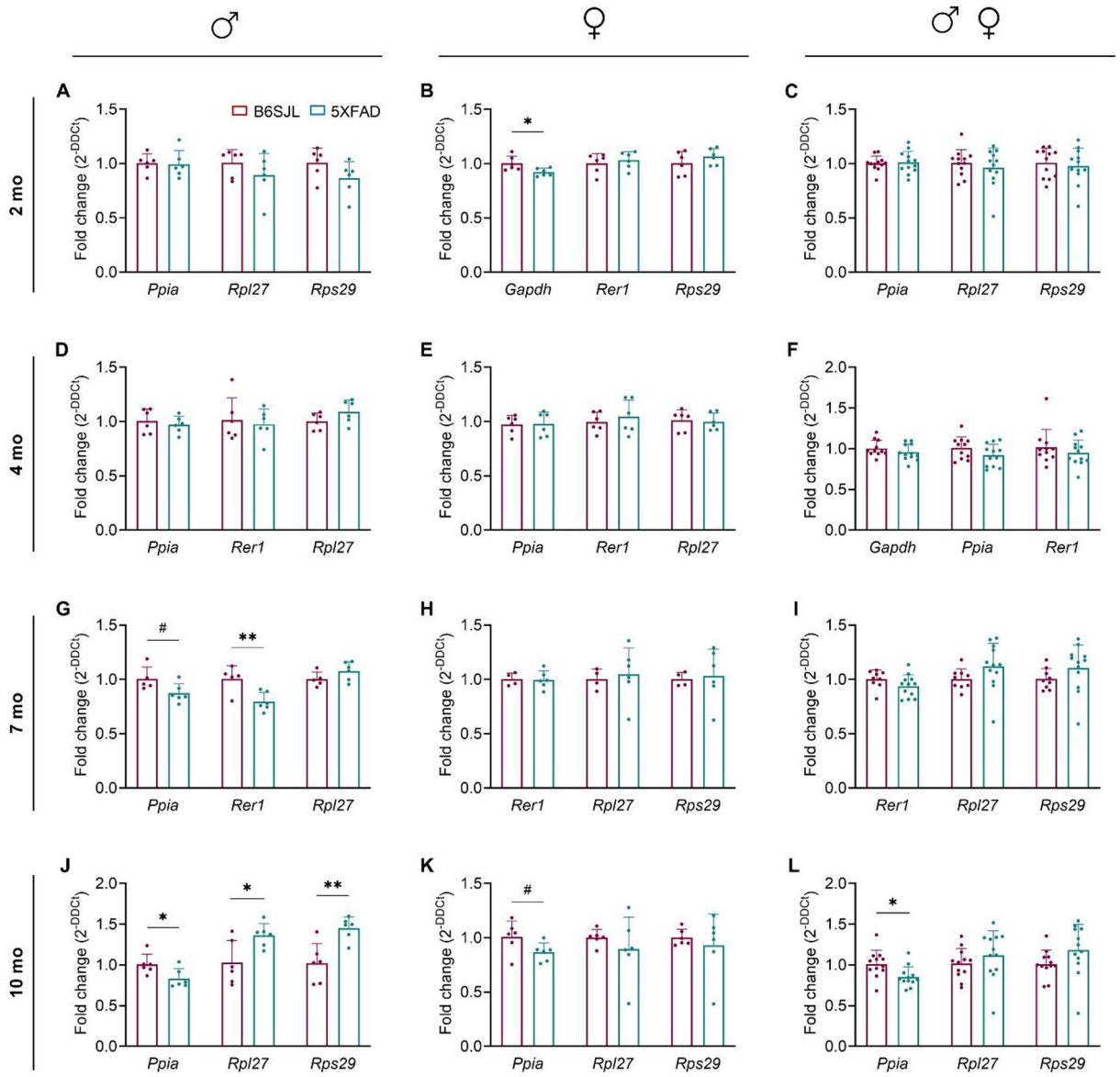

Fig. 3. Effect of genotype on RG expression in the CTX of B6SJL and 5XFAD mice at different ages. B6SJL (2 mo: $n = 6$ M, 6 F; 4 mo: $n = 6$ M, 6 F; 7 mo: $n = 5$ M, 4 F; 10 mo: $n = 5$ M, 6 F) and 5XFAD (2 mo: $n = 6$ M, 6 F; 4 mo: $n = 6$ M, 6 F; 7 mo: $n = 6$ M, 6 F; 10 mo: $n = 6$ M, 6 F) mice were sacrificed at 2, 4, 7 and 10 mo and brains were isolated and dissected. The relative expression of RGs in 5XFAD mice compared to B6SJL controls was determined with the 2MS RGs as internal control as follows: **Male: (A)** 2 mo: *Gapdh - Rer1*; **(D)** 4 mo: *Gapdh - Rps29*; **(G)** 7 mo: *Gapdh - Rps29*; (**J**) 10 mo: *Gapdh - Rer1*. **Female: (B)** 2 mo: *Ppia - Rpl27*; **(E)** 4 mo: *Gapdh - Rps29*; (**H**) 7 mo: *Ppia - Gapdh*; **(K)** 10 mo: *Gapdh - Rer1*. **All animals: (C)** 2 mo: *Gapdh - Rer1*; (**F**) 4 mo: *Rpl27 - Rps29*; (**I**) 7 mo: *Gapdh - Ppia*; **(L)** 10 mo: *Gapdh - Rer1*. For each age, mean Ct values of B6SJL were used as calibrator. Bar graphs show mean fold changed (2^{-DDCt}) values ± SD; burgundy and petrol dots represent, respectively, B6SJL and 5XFAD mice. Statistical analysis was performed according to repeated measure ANOVA with genotype as between factors and RGs (three levels) as within factors; * $p \leq 0.05$, *** $p < 0.001$, **** $p < 0.001$, # $0.05 < p < 0.1$. **Abbreviations**: Ct: cycle threshold; CTX: cerebral cortex; *Gapdh*: glyceraldehyde-3-phosphate dehydrogenase; *Ppia*: peptidylprolyl isomerase A; *Rer1*: retention in endoplasmic reticulum sorting receptor 1; *Rpl27*: ribosomal protein L27; *Rps29*: ribosomal protein S29; SD: standard deviation.

not in the LS (*Mean*: 0.950, $p = 0.474$). This reduction in *Cx3cl1* expression persisted at 10 mo, though with more variability. In males, expression remained significantly reduced (*Mean*: 2MS: 0.827, $p = 0.021$; LS: 0.575, $p = 0.008$; A: 0.754, $p = 0.027$). In females, only the 2MS dataset showed a significant decrease (*Mean*: 0.774, $p = 0.002$), while the LS dataset showed no change (*Mean*: 1.018, $p = 0.625$), and the A RGs analysis did not reach significance (*Mean*: 0.865, $p = 0.102$).

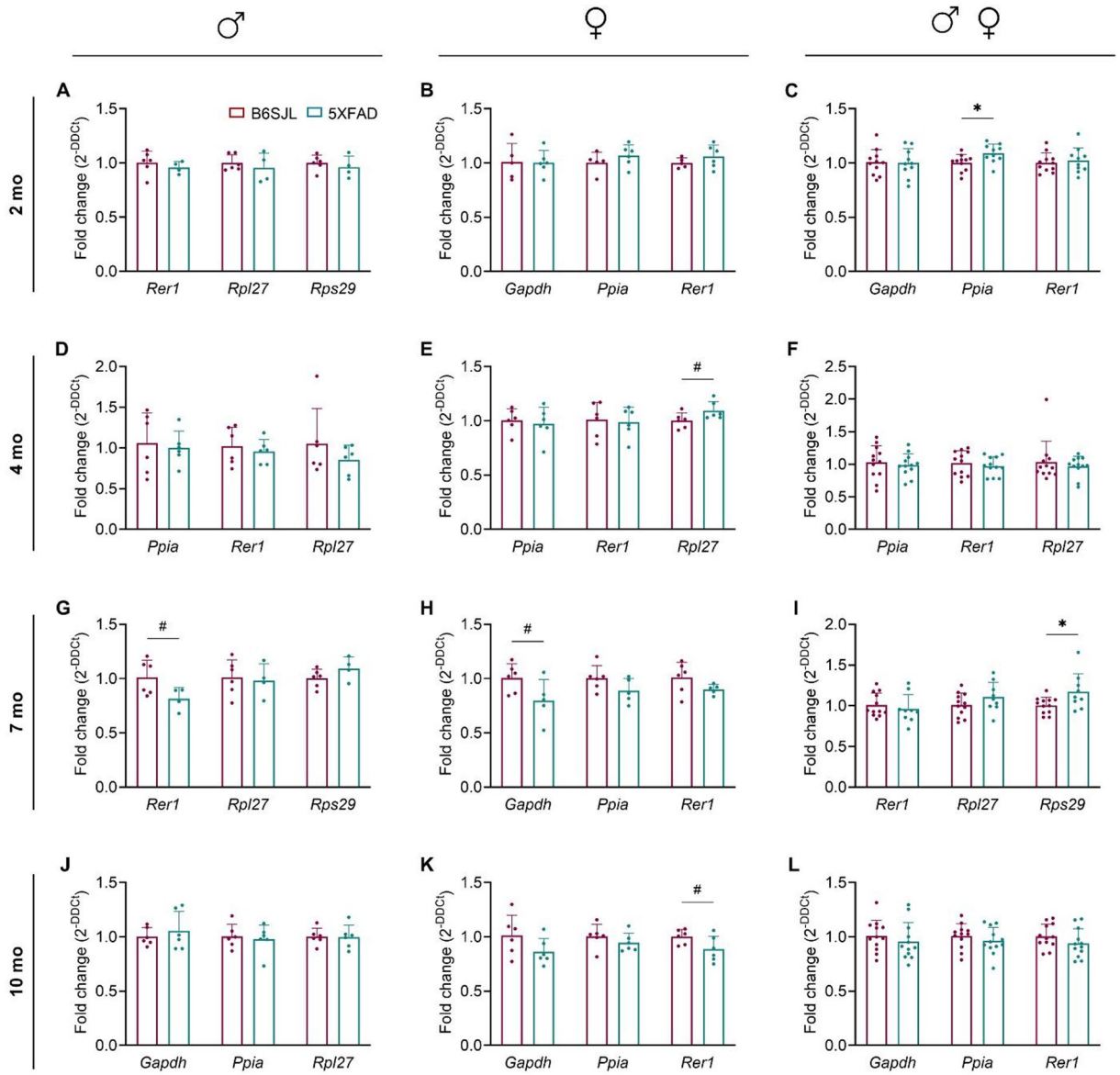

Fig. 4. Effect of genotype on RG expression in the HIPP of B6SJL and 5XFAD mice during AD progression. B6SJL (2 mo: $n = 6$ M, 6 F; 4 mo: $n = 6$ M, 6 F; 7 mo: $n = 5$ M, 4 F; 10 mo: $n = 5$ M, 6 F) and 5XFAD (2 mo: $n = 6$ M, 6 F; 4 mo: $n = 6$ M, 6 F; 7 mo: $n = 6$ M, 6 F; 10 mo: $n = 6$ M, 6 F) mice were sacrificed at 2, 4, 7 and 10 mo and brains were isolated and dissected. The relative expression of RGs in 5XFAD mice compared to B6SJL controls was determined with the 2MS RGs as internal control as follows: **Male: (A)** 2 mo: *Gapdh - Ppia*; **(D)** 4 mo: *Gapdh - Rps29*; **(G)** 7 mo: *Gapdh - Ppia*; **(J)** 10 mo: *Rps29 - Rer1*. **Female: (B)** 2 mo: *Rpl27 - Rps29*; **(E)** 4 mo: *Gapdh-Rps29*; **(H)** 7 mo: *Rpl27-Rps29*; **(K)** 10 mo: *Rps29-Gapdh*. **All animals: (C)** 2 mo: *Rpl27 - Rps29*; **(F)** 4 mo: *Gapdh - Rps29*; **(I)** 7 mo: *Gapdh - Ppia*; **(L)** 10 mo: *Rpl27 - Rps29*. For each age, mean Ct values of B6SJL were used as calibrator. Data are shown as mean (2^{-DDCt}) values ± SD; burgundy and petrol dots represent, respectively, B6SJL and 5XFAD mice. Statistical analysis was performed according to repeated measure ANOVA with genotype as between factors and RGs (three levels) as within factors; * $p \leq 0.05$, *** $p < 0.001$, **** $p < 0.001$, # $0.05 < p < 0.1$. **Abbreviations**: Ct: cycle threshold; HIPP: hippocampus; *Gapdh*: glyceraldehyde-3-phosphate dehydrogenase; *Ppia*: peptidylprolyl isomerase A; *Rer1*: retention in endoplasmic reticulum sorting receptor 1; *Rpl27*: ribosomal protein L27; *Rps29*: ribosomal protein S29; SD: standard deviation.

Hippocampus

Hexb expression

At 2 mo, *Hexb* expression was significantly increased in female 5XFAD mice in the 2MS ($p = 0.007$) and A ($p = 0.027$) RGs datasets, with a non-significant trend in the LS dataset ($p = 0.094$). No genotype-related differences were observed in male mice at this age. By 4 mo, a clear upregulation was evident in females across all datasets ($p < 0.001$), while males showed significant increases in the LS ($p < 0.001$) and A ($p = 0.014$) RGs datasets and a trend in the 2MS dataset ($p = 0.090$), corresponding to roughly 2.5-fold and 2-fold increases in females and

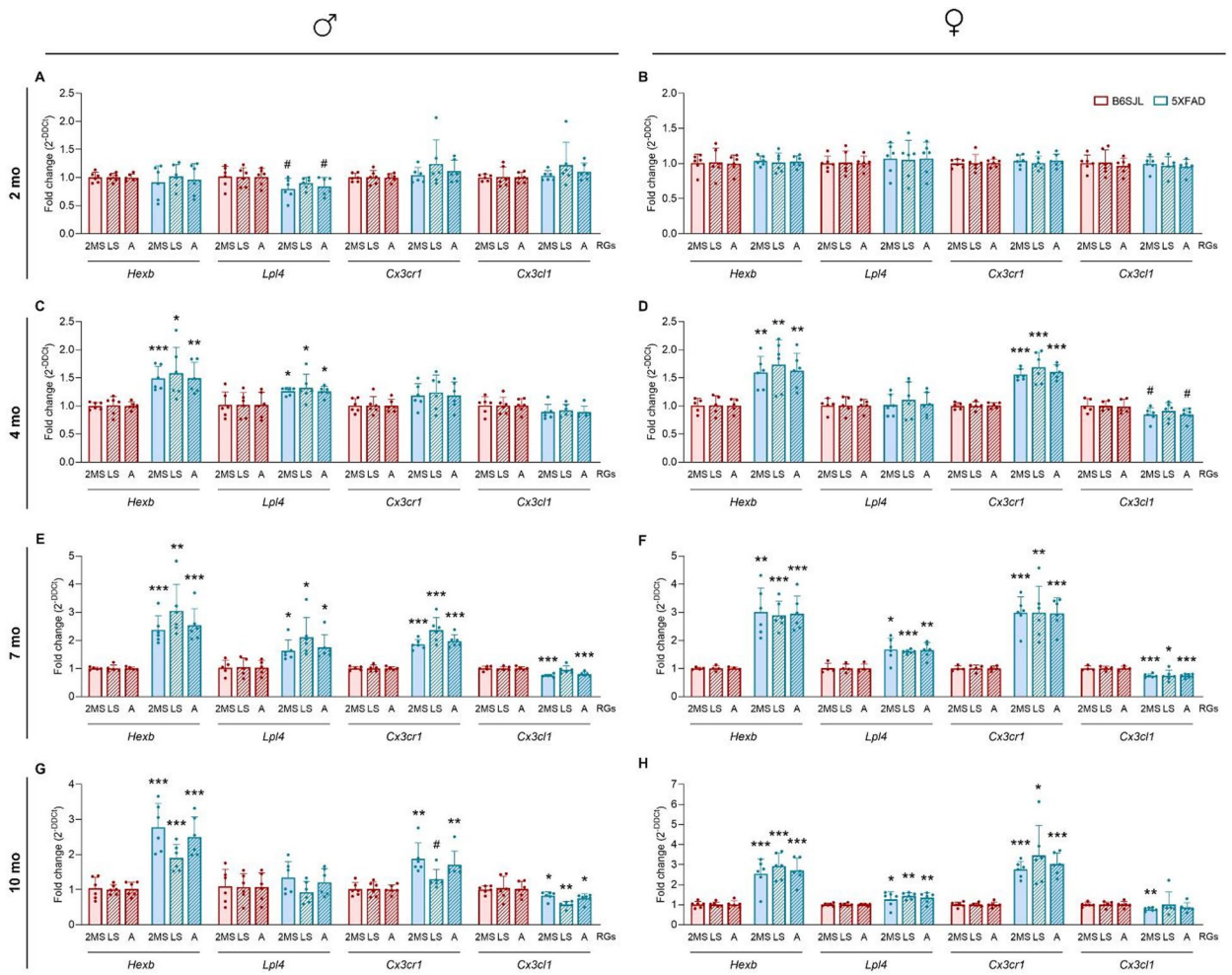

Fig. 5. Temporal expression profiles of *Hexb*, *Lpl4*, *Cx3cr1*, and *Cx3cl1* in CTX of male and female 5XFAD mice, analyzed across 2MS, LS, and A RGs datasets. B6SJL (2 mo: $n = 6$ M, 6 F; 4 mo: $n = 6$ M, 6 F; 7 mo: $n = 5$ M, 4 F; 10 mo: $n = 5$ M, 6 F) and 5XFAD (2 mo: $n = 6$ M, 6 F; 4 mo: $n = 6$ M, 6 F; 7 mo: $n = 6$ M, 6 F; 10 mo: $n = 6$ M, 6 F) mice were sacrificed at 2, 4, 7 and 10 mo and brains were isolated and dissected. The relative expression of *Hexb*, *Lpl4*, *Cx3cr1*, and *Cx3cl1* in 5XFAD mice compared to B6SJL controls was determined with the 2MS, the LS and A RGs as internal control. For each age, mean Ct values of B6SJL were used as calibrator. Bar graphs show mean fold changed (2^{-DDCt}) values ± SD; burgundy and petrol dots represent, respectively, B6SJL and 5XFAD mice. Statistical analysis was performed according to univariate ANOVA; * $p \leq 0.05$, *** $p < 0.001$, **** $p < 0.001$, # $0.05 < p < 0.1$. **Abbreviations**: 2MS: 2 most stable; A: all, Ct: cycle threshold; *Cx3cr1*: C-X3-C motif chemokine receptor 1; *Cx3cl1*: C-X3-C motif chemokine ligand 1; *Hexb*: hexosaminidase B; *Lpl4*: lipoprotein lipase 4; LS: least stable; RGs: reference genes; SD: standard deviation.

males, respectively. This upregulation was intensified at 7 mo, with males exhibiting significant increases (*Mean*: 2MS: 2.644-fold, $p = 0.014$; LS: 3.249-fold, $p = 0.004$; A RGs: 2.709-fold, $p = 0.007$) and females showing even higher elevations (*Mean*: 2MS: 3.843-fold, LS: 4.390-fold, A: 4.241-fold; all $p < 0.001$). At 10 mo, *Hexb* expression remained significantly elevated in both males (*Mean*: 2MS: 3.524-fold, LS: 3.688-fold, A: 3.526-fold; all $p < 0.001$) and females (*Mean*: 2MS: 3.891-fold, LS: 4.414-fold, A: 4.160-fold; all $p < 0.001$). Overall, *Hexb* expression in 5XFAD mice demonstrated a progressive and sustained elevation starting early in females and becoming more prominent in both sexes with disease progression.

Lpl4 expression

Lpl4 expression remained largely unchanged across time points in 5XFAD mice. No significant genotype-related differences were detected; the only exception was a significant decrease in female 5XFAD mice in 2MS datasets.

Cx3cr1 expression

Cx3cr1 expression remained largely unchanged across earlier time points in 5XFAD mice. At 4 mo, *Cxc3cr1* expression was moderately increased in 5XFAD mice compared to controls. In male mice, this upregulation reached significance in the LS dataset (*Mean*: 1.673-fold, $p = 0.017$). In contrast, female mice showed a significant increase across all datasets (*Mean*: 2MS: 2.141-fold, $p = 0.002$; LS: 2.128-fold, $p < 0.001$; A: 2.097-fold, $p < 0.001$),

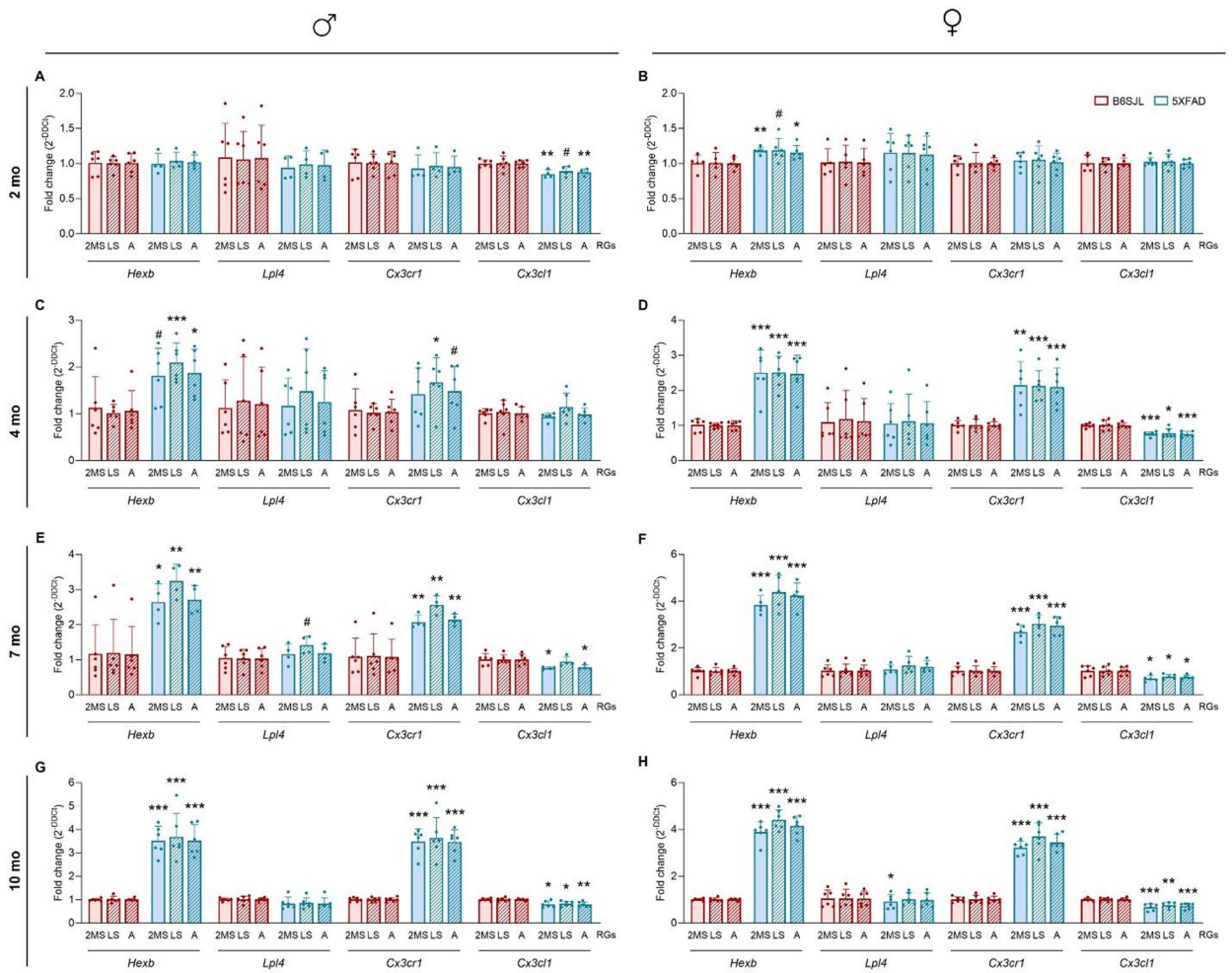

Fig. 6. Temporal expression profiles of *Hexb*, *Lpl4*, *Cx3cr1*, and *Cxc3l1* in the HIPP of male and female 5XFAD mice, analyzed across 2MS, LS, and A RGs datasets. B6SJL (2 mo: $n = 6$ M, 6 F; 4 mo: $n = 6$ M, 6 F; 7 mo: $n = 5$ M, 4 F; 10 mo: $n = 5$ M, 6 F) and 5XFAD (2 mo: $n = 6$ M, 6 F; 4 mo: $n = 6$ M, 6 F; 7 mo: $n = 6$ M, 6 F; 10 mo: $n = 6$ M, 6 F) mice were sacrificed at 2, 4, 7 and 10 mo and brains were isolated and dissected. The relative expression of *Hexb*, *Lpl4*, *Cx3cr1*, and *Cx3cl1* in 5XFAD mice compared to B6SJL controls was determined with the 2MS, the LS and A RGs as internal control. For each age, mean Ct values of B6SJL were used as calibrator. Bar graphs show mean fold changed (2^{-DDCt}) values ± SD; burgundy and petrol dots represent, respectively, B6SJL and 5XFAD mice. Statistical analysis was performed according to univariate ANOVA; * $p \leq 0.05$, *** $p < 0.001$, **** $p < 0.001$, # $0.05 < p < 0.1$. **Abbreviations**: 2MS: 2 most stable; A: all, Ct: cycle threshold; *Cx3cr1*: C-X3-C motif chemokine receptor 1; *Cx3cl1*: C-X3-C motif chemokine ligand 1; H*exb*: hexosaminidase B glyceraldehyde-3-phosphate dehydrogenase; *Lpl4*: lipoprotein lipase 4; LS; least stable; SD: standard deviation.

indicating a more robust genotype effect in females at this time point. At 7 mo, the upregulation of *Cx3cr1* expression became more pronounced in both sexes. In males, expression increased to 2.076-fold ($p = 0.008$) in the 2MS dataset, 2.570-fold ($p = 0.002$) in the LS dataset, and 2.139-fold ($p = 0.004$) in the A dataset. Female mice showed even higher levels in all datasets (2MS: 2.675, $p < 0.001$; LS: 3.035, $p < 0.001$; A: 2.950, $p < 0.001$). By 10 mo, *Cx3cr1* expression remained significantly elevated in both male and female 5XFAD mice. In males, fold changes were similar across all datasets (*Mean*: 2MS: 3.482, LS: 3.637, A: 3.474; all $p < 0.001$), indicating consistent upregulation. Similarly, females maintained high expression levels (*Mean*: 2MS: 3.220, LS: 3.691, A: 3.450; all $p < 0.001$).

Cx3cl1 expression

At 2 mo, *Cx3cl1* expression was significantly decreased in male 5XFAD mice, with reductions observed in the 2MS (*Mean*: 0.851-fold, $p = 0.002$) and A RGs (*Mean*: 0.875-fold, $p = 0.004$) datasets, while the LS dataset showed a non-significant trend (*Mean*: 0.890-fold, $p = 0.092$). In contrast, female mice showed no significant changes at this time point. At 4 mo, the pattern reversed and no significant differences were detected in males, whereas females exhibited a significant reduction across all datasets (*Mean*: 2MS: 0.755-fold, $p < 0.001$; LS: 0.777-fold, $p = 0.017$; A: 0.752-fold, $p < 0.001$), suggesting the onset of genotype effects in females at this stage. By 7 mo, the downregulation of *Cx3cl1* further increased in both sexes. In males, expression remained significantly reduced

in the 2MS (*Mean*: 0.757-fold, $p = 0.019$) and A (*Mean*: 0.783-fold, $p = 0.024$) datasets, but not in the LS dataset (*Mean*: 0.944-fold, $p = 0.488$). Female mice showed a more robust and uniform decrease across all datasets (*Mean*: 2MS: 0.688-fold, $p = 0.015$; LS: 0.775-fold, $p = 0.040$; A: 0.752-fold, $p = 0.016$), reflecting a progressive and generalized suppression of *Cx3cl1* expression. At 10 mo, this downregulation persisted in both sexes. In males, expression remained significantly decreased across all datasets (*Mean*: 2MS: 0.804-fold, $p = 0.011$; LS: 0.826-fold, $p = 0.010$; A: 0.799-fold, $p < 0.001$). Similarly, females maintained a strong reduction in expression (*Mean*: 2MS: 0.682-fold, $p < 0.001$; LS: 0.767-fold, $p = 0.002$; A: 0.726-fold, $p < 0.001$).

Overall, no significant sex- or age-dependent changes in TG expression were observed using any calibrator in B6SJL mice, indicating, on the one hand, the stability in the expression of these genes in control mice during adulthood (2–10 mo), and, on the other hand, the efficacy of any canonical RG in a condition that is neither pathological nor physiologically dynamic or challenging (e.g., development, ageing, environmental enrichment). As regards TG expression in 5XFAD mice, multiple changes in TG expression were detected, especially at later ages. In this case, the choice of calibrator has an impact on TG change detection, being LS normalization often different (not or less significant and more variable) from 2MS and A normalization.

Discussion

The identification of dynamic changes in gene expression represents an important approach for studying the mechanism underlying neurodegenerative diseases. For this study, the 5XFAD model was selected because of its rapid and aggressive amyloid pathology, which enables the study of early disease processes over a condensed timeline[5,17]. Unlike slower-developing models such as 3XTg-AD[28], APP/PS1[29], and Tg2576[30], 5XFAD mice exhibit substantial amyloid accumulation within months, resulting in rapid changes in neuronal and glial transcriptional profiles. These fast molecular alterations can alter the expression level of commonly used RGs, highlighting the need for their context-specific validation in aggressive AD models. The inclusion of the 2, 4, 7 and 10 mo groups allowed us to assess RG expression stability across biologically meaningful stages of 5XFAD disease progression[17,19]. Evaluating RGs across these defined pathological milestones is crucial, because the rapid and aggressive progression of the 5XFAD model can significantly alter cellular composition and molecular homeostasis. Consequently, genes that remain stable at early time points may become dysregulated when neuroinflammation, gliosis, and synaptic alterations intensify. The chosen age points, therefore, provide a structured framework for assessing the reliability of RGs as calibrators of TG expression changes during phases of pathological process acceleration.

For all mentioned reasons, the appropriate normalization of data obtained by RT-qPCR experiment is required to identify possible physiological/pathological differences between tested samples. To ensure the reliability and accuracy of quantitative results, the identification and validation of internal RGs represents a crucial preliminary step to identify at least a couple of genes, whose expression level remains stable in experimental conditions. The use of specific software can assist in the identification of the most stable candidates among a set of RGs.

In this study, after demonstrating global changes in the expression of 5 canonical RGs (Fig. 2), we conducted a systematic analysis of their stability combining results from 4 different software/tools (i.s. NormFinder, GeNorm, Bestkeeper and EndoGene Analyzer), broadly used by the scientific community[25,26,31,32]. We identified the 2MS RGs across multiple experimental groups in both the CTX and HIPP of 5XFAD and control B6SJL mice. Our findings reveal substantial variability in RG stability across regions, ages, and sexes, emphasizing the need for rigorous, context-specific validation of RGs rather than reliance on traditional HKGs alone.

In fact, our main results reinforce the notion that RG stability is not fixed but highly dependent on brain region, sex, and age; the CTX showed more variability in RG combinations, while the HIPP, particularly in females, displayed more consistent stability patterns. *Gapdh* was generally a reliable RG in both regions, especially in male mice and early-to-mid disease stages (2, 4 mo). However, its performance declined in late-stage hippocampal samples in males, highlighting the need for dynamic validation across time points. Other genes like *Rps29*, *Ppia*, *Rpl27*, and *Rer1* emerged as robust co-stable RGs in various contexts, with *Rps29* particularly standing out as a consistently stable partner across brain regions, sexes, and time points. Importantly, *Rpl27* showed remarkable consistency in the female HIPP and all animal analyses, positioning it as a strong candidate for future studies in similar AD models (Tables 2, 3, 4, 5, 6 and 7). Indeed, disease progression is accompained by changes in RG stability. Therefore, even within the same model, each disease-stage must not be considered equal. In fact, the genes identified as the most stable are not the same between all animals group (considering all disease-stages) and single age groups.

Several of the candidate RGs identified as most stable in our dataset - particularly *Gapdh*, *Ppia*, *Rps29*, and *Rpl27* - have been reported in the literature to exhibit variable expression depending on tissue type, age, or disease context, including in AD. For instance, while *Gapdh* remains one of the most commonly used RGs, multiple studies have shown its expression can vary markedly in the brain under pathological conditions such as ischemia, aging, or neurodegeneration[1,7,32–34]. Similarly, ribosomal protein genes such as *Rps29* and *Rpl27* - which we identified as stable in several experimental groups - have been found to be differentially expressed in AD-related proteomic and transcriptomic studies, particularly in brain regions undergoing ribosomal dysfunction. This underlines the risk of using these genes as internal controls without proper validation[35–37]. Conversely, *Ppia* has been consistently reported as a highly stable RG in the CNS, as confirmed by our study, reinforcing its reliability[38,39]. Notably, *Rer1*, although less commonly evaluated in this context, showed stable expression in several groups, suggesting potential as a novel RG candidate for future studies. Overall, our findings align with the broader consensus that RG stability is highly context-dependent and must be empirically validated for each experimental setup, especially in neurodegenerative disease models where molecular changes are widespread and dynamic.

It is noteworthy that some of the genes selected as stable in our dataset (e.g., *Rps29*, *Rpl27*) have been implicated in altered ribosomal/protein-synthesis pathways in neurodegenerative disease (e.g., up-regulation

of ribosomal proteins in AD brain capillaries)[40]. This underlines that their use as RGs in other similar studies should be validated beforehand rather than assumed. Conversely, the strong performance of *Ppia* and *Gapdh* in our dataset is supported by external literature (e.g., *Ppia* among most stable RGs in AD frontal cortex)[38].

To demonstrate the impact of RG selection, for each area/sex/age, the 2 genes identified as most stable (2MS) were used to evaluate the expression of four TGs: *Hexb*, *Lpl4*, *Cx3cr1* and *Cx3cl1*. The results were then compared with data obtained by normalizing over the LS as over A RGs. With minor exceptions, the use of 2MS or A RGs generally leads to smaller SD and higher significance level at the statistical analysis, highlighting once again the critical nature of RG selection in influencing analysis outcome (Figs. 5 and 6).

In summary, our findings emphasize that RG stability cannot be uncritically assumed, particularly in models like 5XFAD, and reinforce the importance of rigorous normalization strategies to obtain reliable gene expression data. Instead, we recommend pairwise normalization using empirically validated RGs, tailored to the specific experimental context, including age, brain region, and sex. Finally, because the 5XFAD model has a particularly aggressive and rapid pathology, the risk that HKGs are perturbed is even greater than in other AD models. However, the method used for this severe model should be also applied for AD models of lower severity and/or with slower disease progression rates, as 3xTg-AD and APP/PS1 mice, where RG expression might also be influence by sex, brain area and disease stage. Thus, our work complements a growing - but still limited - appreciation across the field that RGs must be validated in the specific disease context and at relevant disease stages, especially in neurodegeneration models.

Limitations and future directions

Overall, this study provides a valuable reference for selecting appropriate RGs for transcriptomic analyses in a widely used AD mouse model. Future work should explore whether these stability patterns persist in other brain regions, in later disease stages, or under different experimental manipulations such as drug treatment or behavioral paradigms. Additionally, extending these analyses to other AD models could help determine whether the observed RG dynamics are specific to 5XFAD pathology or more broadly applicable across AD phenotypes. It also provides guidance on the methods to be used when selecting RGs.

This study was limited to a selected panel of candidate RGs; future work should expand this panel and explore transcriptomic datasets to identify novel, even more stable RGs in neurodegenerative settings. Additionally, extending these analyses to other brain regions, different AD mouse models, or human tissues could enhance the translational relevance of our findings.

Data availability

Data are contained within the article and supplementary files.

Received: 6 November 2025; Accepted: 29 January 2026
Published online: 04 February 2026

References

1. Gutala, R. V. & Reddy, P. H. The use of real-time PCR analysis in a gene expression study of alzheimer's disease post-mortem brains. *J. Neurosci. Methods*. **132**(1), 101–107 (2004).
2. Rydbirk, R. et al. Assessment of brain reference genes for RT-qPCR studies in neurodegenerative diseases. *Sci. Rep.* **6**, 37116 (2016).
3. Bagyinszky, E., Giau, V. V. & An, S. A. Transcriptomics in Alzheimer's Disease: Aspects and Challenges. *Int. J. Mol. Sci.* **21**(10), 3517 (2020).
4. Coulson, D. T. et al. Identification of valid reference genes for the normalization of RT qPCR gene expression data in human brain tissue. *BMC Mol. Biol.* **9**, 46 (2008).
5. Oakley, H. et al. Intraneuronal beta-amyloid aggregates, neurodegeneration, and neuron loss in Transgenic mice with five Familial alzheimer's disease mutations: potential factors in amyloid plaque formation. *J. Neurosci.* **26**(40), 10129–10140 (2006).
6. Boda, E. et al. Selection of reference genes for quantitative real-time RT-PCR studies in mouse brain. *J. Mol. Neurosci.* **37**(3), 238–253 (2009).
7. Timaru-Kast, R. et al. Influence of age on cerebral housekeeping gene expression for normalization of quantitative polymerase chain reaction after acute brain injury in mice. *J. Neurotrauma*. **32**(22), 1777–1788 (2015).
8. Janssens, J. et al. Evaluating the applicability of mouse sines as an alternative normalization approach for RT-qPCR in brain tissue of the APP23 model for alzheimer's disease. *J. Neurosci. Methods*. **320**, 128–137 (2019).
9. Ochi, S. et al. Identifying blood transcriptome biomarkers of alzheimer's disease using Transgenic mice. *Mol. Neurobiol.* **57**(12), 4941–4951 (2020).
10. Uppalapati, A., Wang, T. & Nguyen, L. H. Evaluation of suitable reference genes for gene expression studies in the developing mouse cortex using RT-qPCR. *BMC Neurosci.* **26**(1), 12 (2025).
11. Butterfield, D. A., Hardas, S. S. & Lange, M. L. Oxidatively modified glyceraldehyde-3-phosphate dehydrogenase (GAPDH) and alzheimer's disease: many pathways to neurodegeneration. *J. Alzheimers Dis.* **20**(2), 369–393 (2010).
12. Rydbirk, R. et al. Author correction: assessment of brain reference genes for RT-qPCR studies in neurodegenerative diseases. *Sci. Rep.* **10**(1), 12559 (2020).
13. Landel, V. et al. Temporal gene profiling of the 5XFAD Transgenic mouse model highlights the importance of microglial activation in alzheimer's disease. *Mol. Neurodegener.* **9**, 33 (2014).
14. Vasilopoulou, F. et al. Microarray analysis revealed inflammatory transcriptomic changes after LSL60101 treatment in 5XFAD mice model. *Genes (Basel)*. **12**(9), 1315 (2021).
15. Grinan-Ferre, C. et al. Environmental enrichment improves cognitive Deficits, AD hallmarks and epigenetic alterations presented in 5xFAD mouse model. *Front. Cell. Neurosci.* **12**, 224 (2018).
16. Thadathil, N. et al. DNA Double-Strand break accumulation in alzheimer's disease: evidence from experimental models and postmortem human brains. *Mol. Neurobiol.* **58**(1), 118–131 (2021).
17. Daini, E. et al. A regional and cellular analysis of the early intracellular and extracellular accumulation of Abeta in the brain of 5XFAD mice. *Neurosci. Lett.* **754**, 135869 (2021).
18. O'Leary, T. P. & Brown, R. E. Age-related changes in species-typical behaviours in the 5xFAD mouse model of alzheimer's disease from 4 to 16 months of age. *Behav. Brain Res.* **465**, 114970 (2024).

19. Forner, S. et al. Systematic phenotyping and characterization of the 5xFAD mouse model of alzheimer's disease. *Sci. Data*. **8**(1), 270 (2021).
20. Vilella, A. et al. PCSK9 ablation attenuates Abeta pathology, neuroinflammation and cognitive dysfunctions in 5XFAD mice. *Brain Behav. Immun.* **115**, 517–534 (2024).
21. Villacampa, N. et al. Astrocyte-targeted production of IL-10 induces changes in microglial reactivity and reduces motor neuron death after facial nerve axotomy. *Glia* **63**(7), 1166–1184 (2015).
22. Bustin, S. A. et al. The MIQE guidelines: minimum information for publication of quantitative real-time PCR experiments. *Clin. Chem.* **55**(4), 611–622 (2009).
23. Andersen, C. L., Jensen, J. L. & Orntoft, T. F. Normalization of real-time quantitative reverse transcription-PCR data: a model-based variance Estimation approach to identify genes suited for normalization, applied to bladder and colon cancer data sets. *Cancer Res.* **64**(15), 5245–5250 (2004).
24. Vandesompele, J. et al. Accurate normalization of real-time quantitative RT-PCR data by geometric averaging of multiple internal control genes. *Genome Biol.* **3**(7), RESEARCH0034 (2002).
25. Pfaffl, M. W. et al. Determination of stable housekeeping genes, differentially regulated target genes and sample integrity: BestKeeper–Excel-based tool using pair-wise correlations. *Biotechnol. Lett.* **26**(6), 509–515 (2004).
26. Teixeira, E. B. et al. EndoGeneAnalyzer: A tool for selection and validation of reference genes. *PLoS One*. **19**(4), e0299993 (2024).
27. Livak, K. J. & Schmittgen, T. D. Analysis of relative gene expression data using real-time quantitative PCR and the 2(-Delta delta C(T)) method. *Methods* **25**(4), 402–408 (2001).
28. Belfiore, R. et al. Temporal and regional progression of alzheimer's disease-like pathology in 3xTg-AD mice. *Aging Cell.* **18**(1), e12873 (2019).
29. Chintapaludi, S. R. et al. Staging alzheimer's disease in the brain and retina of B6.APP/PS1 mice by transcriptional profiling. *J. Alzheimers Dis.* **73**(4), 1421–1434 (2020).
30. Kawarabayashi, T. et al. Age-dependent changes in brain, CSF, and plasma amyloid (beta) protein in the Tg2576 Transgenic mouse model of alzheimer's disease. *J. Neurosci.* **21**(2), 372–381 (2001).
31. Wang, Q. et al. Stability of endogenous reference genes in postmortem human brains for normalization of quantitative real-time PCR data: comprehensive evaluation using geNorm, NormFinder, and bestkeeper. *Int. J. Legal Med.* **126**(6), 943–952 (2012).
32. Zampieri, M. et al. Validation of suitable internal control genes for expression studies in aging. *Mech. Ageing Dev.* **131**(2), 89–95 (2010).
33. Kang, Y. et al. Evaluation of reference genes for gene expression studies in mouse and N2a cell ischemic stroke models using quantitative real-time PCR. *BMC Neurosci.* **19**(1), 3 (2018).
34. Nadei, O. V. & Agalakova, N. I. Optimal reference genes for RT-qPCR experiments in hippocampus and cortex of rats chronically exposed to excessive fluoride. *Biol. Trace Elem. Res.* **202**(1), 199–209 (2024).
35. Gui, H. et al. Identification of the hub genes in alzheimer's disease. *Comput. Math. Methods Med.* **2021**, p6329041 (2021).
36. Xu, W. et al. Machine learning-based proteomics profiling of ALS identifies downregulation of RPS29 that maintains protein homeostasis and STMN2 level. *Commun. Biol.* **8**(1), 1177 (2025).
37. Hernandez-Ortega, K. et al. Altered machinery of protein synthesis in alzheimer's: from the nucleolus to the ribosome. *Brain Pathol.* **26**(5), 593–605 (2016).
38. Leduc, V. et al. Normalization of gene expression using SYBR green qPCR: a case for paraoxonase 1 and 2 in alzheimer's disease brains. *J. Neurosci. Methods*. **200**(1), 14–19 (2011).
39. Kovalenko, A. A. et al. Identification of reliable reference genes for use in gene expression studies in rat febrile seizure model. *Int. J. Mol. Sci.* **25**(20), 11125 (2024).
40. Suzuki, M. et al. Upregulation of ribosome complexes at the blood-brain barrier in alzheimer's disease patients. *J. Cereb. Blood Flow. Metab.* **42**(11), 2134–2150 (2022).

Acknowledgements

The authors gratefully acknowledge Dr. Daniela Gandolfi (University of Modena and Reggio Emilia) for providing assistance with the mathematical analysis. This contributor was not involved in authorship decisions.

Author contributions

ED, KA, MP; MB: in vivo investigation, data collection, mouse breeding, ex vivo analysis; AV: data collection and curation, formal analysis, study supervision and validation; ED, AV: original draft preparation; KA, MP; MB, MZ: writing - review \& editing; AV: funding acquisition. All authors have read and agreed to the published version of the manuscript.

Funding

This study was supported by PRIN: PROGETTI DI RICERCA DI RILEVANTE INTERESSE NAZIONALE 2022 to AV.

Declarations

Competing interests

The authors declare no competing interests.

Additional information

Supplementary Information The online version contains supplementary material available at https://doi.org/10.1038/s41598-026-38346-5.

Correspondence and requests for materials should be addressed to A.V.